

Vinyl–Vinyl Coupling on Late Transition Metals through C–C Reductive Elimination Mechanism. A Computational Study

Valentine P. Ananikov,^{†,‡} Djamaladdin G. Musaev,^{‡,*} and Keiji Morokuma^{‡,*}

Contribution from the N. D. Zelinsky Institute of Organic Chemistry, RAS, Leninsky Prospect 47, Moscow 117913, Russia, and Cherry L. Emerson Center for Scientific Computation and Department of Chemistry, Emory University, Atlanta, Georgia 30322

Received November 6, 2001

Abstract: A detailed density functional study was performed for the vinyl–vinyl reductive elimination reaction from bis- σ -vinyl complexes $[M(\text{CH}=\text{CH}_2)_2\text{X}_n]$. It was shown that the activity of these complexes decreases in the following order: $\text{Pd}^{\text{IV}}, \text{Pd}^{\text{II}} > \text{Pt}^{\text{IV}}, \text{Pt}^{\text{II}}, \text{Rh}^{\text{III}} > \text{Ir}^{\text{III}}, \text{Ru}^{\text{II}}, \text{Os}^{\text{II}}$. The effects of different ligands X were studied for both platinum and palladium complexes, which showed that activation barriers for C–C bond formation reaction decrease in the following order: $\text{X} = \text{Cl} > \text{Br}, \text{NH}_3 > \text{I} > \text{PH}_3$. Steric effects induced either by the ligands X or by substituents on the vinyl group were also examined. In addition, the major factors responsible for stereoselectivity control on the final product formation stage and possible involvement of asymmetric coupling pathways are reported. In all cases ΔE , ΔH , ΔG , and ΔG_{aq} energy surfaces were calculated and analyzed. The solvent effect calculation shows that in a polar medium halogen complexes may undergo a reductive elimination reaction almost as easily as compounds with phosphine ligands.

Introduction

Vinyl–vinyl coupling opens a conventional route to conjugated 1,3-dienes and is widely employed in many catalytic coupling reactions.^{1–12} In particular, the palladium-catalyzed Stille reaction,^{3,4,6} Suzuki–Miyaura coupling,⁷ and other cross-coupling schemes^{8,9} have found numerous applications in modern synthesis. Some of the methods became well-established

tools in natural product and new compound synthesis,^{1,3,7} while the great potential of the field is still under continuous development.^{10,11} Another interesting example of the vinyl–vinyl coupling has recently been reported as a part of a platinum-catalyzed stereo- and regioselective alkyne conversion reaction into 1,3-dienes.¹² The reductive elimination step is usually assumed to be a key bond-forming and product-releasing stage of the catalytic cycles.^{1–12}

Although vinyl–vinyl coupling has found widespread practical applications, the mechanism of the process is not well rationalized. Recently, we have investigated the potential energy surface of catalytic conversion reaction of alkynes into 1,3-dienes on a Pt^{IV} center, which involves a C–C reductive elimination stage of two vinyl ligands.¹³ The study clearly indicated that vinyl–vinyl reductive elimination has many peculiarities compared to processes involving alkyl groups. In certain cases, the latter reactions may be taken as a general model for vinyl–vinyl coupling. However, to elucidate the mechanism of metal-assisted C–C bond formation between unsaturated vinyl units, specific consideration of the bis-vinyl system is required. Undoubtedly, deep understanding of the

[†] Zelinsky Institute.

[‡] Emory University.

- (1) *Metal-Catalyzed Cross-Coupling Reactions*; Diederich, F., Stang, P. J., Eds.; Wiley-VCH: Weinheim, Germany, 1998.
- (2) Tsuji, J. *Palladium Reagents and Catalysts: Innovation in Organic Synthesis*; Wiley & Sons: Chichester, U.K., 1995.
- (3) Stille, J. K. *Angew. Chem., Int. Ed. Engl.* **1986**, *25*, 508.
- (4) Farina, V.; Krishnamurthy, V.; Scott, W. J. The Stille Reaction. In *Organic Reactions*; John Wiley & Sons Inc.: New York, 1997; Vol. 50, p 3.
- (5) Beletskaya, I. P. *J. Organomet. Chem.* **1983**, *250*, 551.
- (6) (a) Farina, V.; Krishnamurthy, V.; Scott, W. J. *J. Org. React.* **1997**, *50*, 1 (b) Stille, J. K.; Groh, B. L.; *J. Am. Chem. Soc.* **1987**, *109*, 813.
- (7) (a) Suzuki, A. *J. Organomet. Chem.* **1999**, *576*, 147. (b) Miyaura, N.; Suzuki, A. *Chem. Rev.* **1995**, *95*, 2457. (c) Suzuki, A. In *Metal-Catalyzed Cross-Coupling Reactions*; Diederich, F., Stang, P. J., Eds.; VCH: Weinheim, Germany, 1998; pp 49–97.
- (8) (a) Negishi, E. *Acc. Chem. Res.* **1982**, *15*, 340. (b) Negishi, E.; Takahashi, T.; Akiyoshi, K. *J. Organomet. Chem.* **1987**, *334*, 181. (c) Ritter, K. *Synthesis* **1993**, 735. (d) Tamao, K.; Kobayashi, K.; Ito, Y. *Tetrahedron Lett.* **1989**, *30*, 6051. (e) Hatanaka, Y.; Hiyama, T. *J. Org. Chem.* **1988**, *53*, 918.
- (9) Brandsma, L.; Vasilevsky, S. F.; Verkrujisse, H. D. *Application of Transition Metal Catalysts in Organic Synthesis*; Springer-Verlag: Berlin, 1998.
- (10) For some recent examples of vinyl–vinyl coupling, see: (a) Gallagher, W. P.; Terstiege, I.; Maleczka, R. E. *J. Am. Chem. Soc.* **2001**, *123*, 3194. (b) Maleczka, R. E.; Gallagher, W. P.; Terstiege, I. *J. Am. Chem. Soc.* **2000**, *122*, 384. (c) Caline, C.; Pattenden, G. *Synlett* **2000**, 1661. (d) Kim, H.-O.; Ogbu, C. O.; Nelson, S.; Kahn, M. *Synlett* **1998**, 1059. (e) Ma, Y.; Huang, X. *J. Chem. Soc., Perkin Trans.* **1997**, 2953. (f) Panek, J. S.; Hu, T. *J. Org. Chem.* **1997**, *62*, 4912. (g) Alcaraz, L.; Taylor, R. J. K. *Synlett* **1997**, 791. (h) Jang, S. B. *Tetrahedron Lett.* **1997**, *38*, 1793. (i) Yang, D. Y.; Huang, X. *J. Organomet. Chem.* **1997**, *543*, 165. (j) Allred, G. D.; Liebeskind, L. S. *J. Am. Chem. Soc.* **1996**, *118*, 2748.
- (11) C–C cross coupling catalyzed by palladium complexes with nitrogen ligands: (a) van Asselt, R.; Elsevier, C. *J. Organometallics* **1994**, *13*, 1972. (b) van Asselt, R.; Elsevier, C. *J. Tetrahedron* **1994**, *50*, 323.

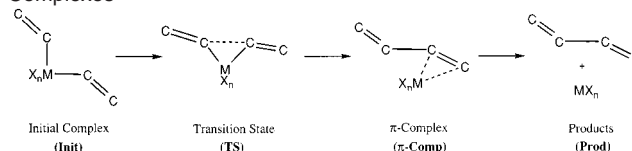
- (12) (a) Ananikov, V.; Mitchenko, S. A.; Beletskaya, I. P. *J. Organomet. Chem.* **2000**, *604*, 290. (b) Ananikov V. P., Ph.D. Thesis, N. D. Zelinsky Institute of Organic Chemistry, Moscow, 1999. (c) Ananikov, V.; Mitchenko, S. A.; Beletskaya, I. P.; Nefedov, S. E.; Eremenko, I. L. *Inorg. Chem. Commun.* **1998**, *1*, 411. (d) Mitchenko, S. A.; Ananikov V. P.; Beletskaya, I. P.; Ustynyuk, Y. A. *Mendeleev Commun.* **1997**, *4*, 130.
- (13) Ananikov, V. P.; Musaev, D. G.; Morokuma, K. *Organometallics* **2001**, *20*, 1652.
- (14) (a) *Comprehensive Asymmetric Catalysis*; Jacobsen, E. N., Pfaltz, A., Yamamoto, H., Eds.; Springer: Berlin, 1999. (b) *Applied Homogeneous Catalysis with Organometallic Compounds*; Corlins, B., Herrman, W. A., Eds.; VCH: Weinheim, Germany, 1996. (c) *Asymmetric Catalysis in Organic Synthesis*; Noyori, R., Ed.; Wiley: New York, 1994. (d) Kagan, H. B. *Asymmetric Synthesis Using Organometallic Catalysts*. In *Comprehensive Organometallic Chemistry*; Wilkinson, G., Stone, F. G. A., Abel, E. W., Eds.; Pergamon Press: Oxford, U.K., 1982, Vol. 8, pp 463–498.

reaction mechanism is a prerequisite for rational design of better catalytic cycles, especially to fulfill modern requirements in asymmetric synthesis.¹⁵

Transition metal σ -vinyl derivatives may be prepared in a number of well-developed ways^{12,15,17–20} and bis- σ -vinyl compounds are equally well known.¹⁶ Not surprisingly, C–C bond formation through vinyl–vinyl reductive elimination has been used not only inside the catalytic cycles but also as a stoichiometric reaction starting from bis- σ -vinyl complexes of Pt^{IV},¹² Rh^{III},¹⁷ Ir^{III},¹⁸ Ru^{II},^{19,20} and Os^{II}.¹⁹

Numerous mechanistic studies on C–C reductive elimination and reverse process, oxidative addition (C–C bond activation) have been published for dialkyl or mixed complexes of platinum,^{21–27} palladium,^{24,28} rhodium,²⁶ ruthenium,²⁵ and iridium.²⁶ Several theoretical investigations on C–C bond activation by platinum,^{29–32} palladium,^{29,30,32,33} rhodium,^{33–36} and iridium^{35,37} have been also performed with various methods, recently in many cases at DFT³¹ or ONIOM (DFT:HF)

Scheme 1. Vinyl–Vinyl Coupling Reaction on Transition Metal Complexes



levels.^{34,35} However, these studies were made for C_{sp3}–C_{sp3} and C_{sp3}–C_{aryl} (in most cases methyl–methyl and methyl–aryl, respectively) bonds, and no theoretical study appears to have been carried out for reductive elimination of unsaturated vinyl ligands leading to a conjugated product.

While the number of practical applications involving palladium complexes as catalysts significantly exceeds that reported for platinum,^{1–10} the mechanistic studies more often are performed on the latter metal.^{21–28} This is mainly because of the larger relative stability of organometallic intermediates for platinum derivatives.^{21,22,27,30} This imposes several difficulties in studying palladium systems, to establish factors responsible for tuning catalytic activity and selectivity and to rationalize main features that impart the system with unique properties.

In the present article, we report a density functional study of the mechanism of vinyl–vinyl C–C reductive elimination reaction in the complexes [M(CH=CH₂)₂X_n] (Scheme 1). At first, detailed comparative study of platinum and palladium complexes will be performed with a representative set of ligands (X = Cl, Br, I, NH₃, PH₃) in both M^{II} and M^{IV} oxidation states. Then, we will extend our studies to the complexes of other late transition metals (Rh^{III}, Ir^{III}, Ru^{II}, Os^{II}). In all cases, ΔE , ΔH , ΔG , and ΔG_{aq} will be presented and discussed. Special attention will be paid to the stereoselectivity control of (E/E)-, (Z/E)-, and (Z/Z)-diene product formation. Here we also address the question of possible application of vinyl–vinyl coupling in asymmetric catalysis.

Calculation Procedure

Geometries of the reactants, intermediates, transition states (TSS), and products were optimized using the B3LYP hybrid density functional method.^{38–40} Unless otherwise stated, the standard 6-311G(d,p) basis set⁴¹ for C, N, P, and H and the triple- ζ basis set with the Stuttgart/Dresden effective core potentials^{42–45} (SDD) for halogens (Cl, Br, I)

- (15) (a) Anderson G. K. Platinum–Carbon σ -Bonded Complexes. In *Comprehensive Organometallic Chemistry II*; Abel, E. W., Stone, F. G. A., Wilkinson, G., Eds.; Pergamon Press: Oxford, U.K., 1995, Vol. 9, pp 431–531. (b) Canty, A. J. Palladium–Carbon σ -Bonded Complexes. In *Comprehensive Organometallic Chemistry II*; Abel, E. W., Stone, F. G. A., Wilkinson, G., Eds.; Pergamon Press: Oxford, U.K., 1995, Vol. 9, pp 225–290. (c) Hackett, M.; Whitesides, G. M. *J. Am. Chem. Soc.* **1988**, *110*, 1449. (d) Sebald, A.; Wrackmeyer, B. *J. Chem. Soc., Chem. Commun.* **1983**, 309. (e) Kelley, E. A.; Maitlis, P. M. *J. Chem. Soc., Dalton Trans.* **1979**, 167. (f) Bell, R. A.; Chisholm, M. H. *J. Chem. Soc., Chem. Commun.* **1976**, 200. (g) Mann, B. E.; Bailey, P. M.; Maitlis, P. M. *J. Am. Chem. Soc.* **1974**, *97*, 1275. (h) Chaudhuri, N.; Kekre, M. G.; Puddephatt, R. *J. Organomet. Chem.* **1974**, *73*, C17. (i) Clark, H. C.; Dixon, K. R.; Jacobs, W. *J. Am. Chem. Soc.* **1968**, *90*, 2259.
- (16) For example, see the preparation of [Pt(CH=CH₂)₂{As(CH=CHCl)₃}]₂: Mann, F. G.; Pope, W. *J. Chem. Soc.* **1922**, 121, 1754.
- (17) Wang, Z. Q.; Turner, M. L.; Kunicki, A. R.; Maitlis, P. M. *J. Organomet. Chem.* **1995**, *488*, C11.
- (18) Chin, C. S.; Cho, H.; Won, G.; Oh, M.; Ok, K. M. *Organometallics* **1999**, *18*, 4810.
- (19) Bohanna, C.; Esteruelas, M. A.; Lahoz, F. J.; Onate, E.; Oro, L. A.; Sola, E. *Organometallics* **1995**, *14*, 4825.
- (20) Burn, M. J.; Fickes, M. G.; Hollander, F. J.; Bergman, R. G. *Organometallics* **1995**, *14*, 137.
- (21) Collman, J. P.; Hegedus, L. S.; Norton, J. R.; Finke, R. G. *Principles and Application of Organotransition Metal Chemistry*; University Science Books: Mill Valley, CA, 1987.
- (22) Parshall, G. W.; Ittel, S. D. *Homogeneous Catalysis: The Applications and Chemistry of Catalysis by Soluble Transition Metal Complexes*, 2nd ed.; Wiley-Interscience: New York, 1992.
- (23) (a) Williams, B. S.; Goldberg, K. I. *J. Am. Chem. Soc.* **2001**, *123*, 2576. (b) Crumpton, D. M.; Goldberg, K. I. *J. Am. Chem. Soc.* **2000**, *122*, 962. (c) Hill, G. S.; Yap, G. P. A.; Puddephatt, R. *J. Organometallics* **1999**, *18*, 1408. (d) Albrecht, M.; Gossage, R. A.; Spek, A. L.; van Koten, G. *J. Am. Chem. Soc.* **1999**, *121*, 11898. (e) Hill, G. S.; Puddephatt, R. *J. Organometallics* **1997**, *16*, 4522. (f) Goldberg, K. I.; Yan, J. Y.; Breitung, E. M. *J. Am. Chem. Soc.* **1995**, *117*, 6889. (g) Goldberg, K. I.; Yan, J. Y.; Winter, E. L. *J. Am. Chem. Soc.* **1994**, *116*, 1573. (h) Brown, M. P.; Puddephatt, R. J.; Upton, C. E. *J. Chem. Soc., Dalton Trans.* **1974**, 2457. (i) Appleton, T. G.; Clark, H. C.; Manzer, L. E. *J. Organomet. Chem.* **1974**, *65*, 275. (j) Ruddick, J. D.; Shaw, B. L. *J. Chem. Soc. A* **1969**, 2969. (k) Chatt, J.; Shaw, B. L. *J. Chem. Soc.* **1959**, 705.
- (24) Baylar, A.; Canty, A. J.; Edwards, P. G.; Sletton, B. W.; White, A. H. *J. Chem. Soc., Dalton Trans.* **2000**, 3325.
- (25) Van der Boom, M. E.; Kraatz, H.-B.; Hassner, L.; Ben-David, Y.; Milstein, D. *Organometallics* **1999**, *18*, 3873.
- (26) Rybtchinski, B.; Milstein, D. *Angew. Chem., Int. Ed.* **1999**, *38*, 870 and references therein.
- (27) Rendina, L. M.; Puddephatt, R. J.; *Chem. Rev.* **1997**, *97*, 1735.
- (28) (a) Reid, S. M.; Mague, J. T.; Fink, M. J. *J. Am. Chem. Soc.* **2001**, *123*, 4081. (b) Moravskiy, A.; Stille, J. K. *J. Am. Chem. Soc.* **1981**, *103*, 4182. (c) Loar, M. K.; Stille, J. K.; *J. Am. Chem. Soc.* **1981**, *103*, 4174. (d) Ozawa, F.; Ito, T.; Nakamura, Y.; Yamamoto, A. *Bull. Chem. Soc. Jpn.* **1981**, *54*, 1868. (e) Gillie, A.; Stille, J. K. *J. Am. Chem. Soc.* **1980**, *102*, 4933.
- (29) Tatsumi, K.; Hoffmann, R.; Yamamoto, A.; Stille, J. K. *Bull. Chem. Soc. Jpn.* **1981**, *54*, 1857.
- (30) (a) Low, J. L.; Goddard, W. A. *J. Am. Chem. Soc.* **1986**, *108*, 6115. (b) Low, J. L.; Goddard, W. A. *Organometallics* **1986**, *5*, 609.
- (31) Hill, G. S.; Puddephatt, R. *J. Organometallics* **1998**, *17*, 1478.
- (32) (a) Sakaki, S.; Mizoe, N.; Musashi, Y.; Biswas, B.; Sugimoto, M. *J. Phys. Chem. A* **1998**, *102*, 8027. (b) Sakaki, S.; Ogawa, M.; Musashi, Y.; Arai, T. *Inorg. Chem.* **1994**, *33*, 1660. (c) Sakaki, S.; Ieki, M. *J. Am. Chem. Soc.* **1993**, *115*, 2373.

- (33) (a) Siegbahn, P. E. M.; Blomberg, M. R. A. In *Theoretical Aspects of Homogeneous Catalysis, Applications of Ab Initio Molecular Orbital Theory*; van Leeuwen, P. W. N. M., van Lenthe, J. H., Morokuma, K., Eds.; Kluwer Academic Publishers: Dordrecht, The Netherlands, 1995. (b) Siegbahn, P. E. M.; Blomberg, M. R. A. *J. Am. Chem. Soc.* **1992**, *114*, 10548. (c) Blomberg, M. R. A.; Siegbahn, P. E. M.; Nagashina, U.; Wennerberg, J. *J. Am. Chem. Soc.* **1991**, *113*, 424.
- (34) (a) Sundermann, A.; Uzan, O.; Martin, J. M. L. *Organometallics* **2001**, *20*, 1783. (b) Sundermann, A.; Uzan, O.; Milstein, D.; Martin, J. M. L. *J. Am. Chem. Soc.* **2000**, *122*, 7095.
- (35) Cao, Z.; Hall, M. B. *Organometallics* **2000**, *19*, 3338.
- (36) Koga, N.; Morokuma, K. *Organometallics* **1991**, *10*, 946.
- (37) Krogh-Jespersen, K.; Goldman, A. S. In *Transition State Modeling for Catalysis*; Truhlar, D. G., Morokuma, K., Eds.; ACS Symposium Series 721; American Chemical Society: Washington, DC, 1999; pp 151–162.
- (38) Becke, A. D. *Phys. Rev. A* **1988**, *38*, 3098.
- (39) Lee, C.; Yang, W.; Parr, R. G. *Phys. Rev. B* **1988**, *37*, 785.
- (40) Becke, A. D. *J. Chem. Phys.* **1993**, *98*, 5648.
- (41) (a) Krishnan R.; Binkley, J. S.; Seeger, R.; Pople, J. A. *J. Chem. Phys.* **1980**, *72*, 650. (b) McLean, A. D.; Chandler, G. S. *J. Chem. Phys.* **1980**, *72*, 5639.
- (42) Schwerdtfeger, P.; Dolg M.; Schwarz, W. H.; Bowmaker, G. A.; Boyd, P. D. W. *J. Chem. Phys.* **1989**, *91*, 1762.
- (43) Dolg, M. Ph.D. Thesis, Universitat Stuttgart, 1989.
- (44) Andrae, D.; Haubermann, U.; Dolg, M.; Stoll, H.; Preub, H. *Theor. Chim. Acta* **1990**, *77*, 123.
- (45) Bergner, A.; Dolg M.; Kÿchle, W.; Stoll, H.; Preuss, H. *Mol. Phys.* **1993**, *80*, 1431.

and metals (Pt, Pd, Ir, Rh, Os, Ru) were used in these calculations (further referred as BSI). Normal coordinate analysis has been performed for all stationary points to characterize the TSs (one imaginary frequency) and equilibrium structures (no imaginary frequency) and to calculate zero point energy correction (ZPC) and Gibbs free energies (at 298.15 K, 1 atm).

In our previous work on a similar system,¹³ we established that polarization d functions on halogen atoms does not significantly change the geometry of the transition metal complexes of interest. Here, to elucidate the role of these polarization d functions to the calculated energetics, we performed additional single point energy calculations with a d function on iodine atoms for the reactant, transition state, intermediate, and product of the vinyl–vinyl coupling reaction for $[\text{Pt}(\text{CH}=\text{CH}_2)_2\text{I}_2]^{2-}$ ($M = \text{Pt}$, $X = \text{I}$ and $n = 2$ according to Scheme 1; details will be discussed below). The relative energies, 0.0, 30.8, –12.8, and 10.2 kcal/mol, obtained with the SDD(d) basis set⁴⁶ on iodine only slightly differ from those, 0.0, 31.2, –12.3, and 13.0 kcal/mol, of the SDD basis set, for initial compound, TS, π -complex, and product, respectively. Therefore, below we will not include the d function on halogen atoms in the calculations. However, reduction of the 6-311G(d) basis set to SDD for phosphorus resulted in more significant discrepancies in the calculated energetics. Particularly, full geometry optimization of the reductive elimination reaction from $[\text{Pt}(\text{CH}=\text{CH}_2)_2(\text{PH}_3)_2]$ ($M = \text{Pt}$, $X = \text{PH}_3$, and $n = 2$) gives the relative energies of 0.0, 19.3, –27.4, and –17.8 kcal/mol with 6-311G(d) and 0.0, 21.4, –23.8, and –12.5 kcal/mol with SDD, for the initial compound, TS, π -complex, and product, respectively. Therefore, we decided to keep the 6-311G(d) basis set for phosphorus and nitrogen atoms throughout this work.

To take into account the possible solvent effect of polar media for the reaction of interest, we have performed the polarized-continuum-model (PCM)^{47–53} energy calculations modeling the water environment. In these calculations, we used the B3LYP/BSI optimized geometries; i.e., we did not reoptimize the structures in the presence of solvent since previously it was shown that reoptimization of the geometry has very limited effect on the computed solvation energies.^{54–58} All PCM calculations were carried out at 298.15 K using an average tessera area^{13,55} of 0.4 Å². To make a reliable comparison with gas-phase ΔG values, a thermal correction to free energy from the gas-phase frequency runs was added to the total free energy in solvent calculated with PCM.

Metal–carbon bond dissociation energies (BDE), $D(\text{M}–\text{C})$, were calculated using the relationship

$$\Delta H = 2D(\text{M}–\text{C}) - D(\text{C}–\text{C})$$

where ΔH is the calculated reaction enthalpy, $D(\text{M}–\text{C})$ is the metal–carbon BDE and $D(\text{C}–\text{C})$ is the carbon–carbon single bond dissociation energy in buta-1,3-diene. Since the B3LYP/BSI calculated $D(\text{C}–\text{C}) = 109.7$ kcal/mol is ~ 4 kcal/mol smaller than 115.8 (G2) and 115.7 (experimental) kcal/mol,⁵⁹ the $D(\text{M}–\text{C})$ value we calculate at the B3LYP/BSI level will intrinsically contain an error of -2 kcal/mol, in addition to the error in ΔH . Note that the reaction enthalpy ΔH will be calculated relative to the point of complete dissociation of buta-1,3-diene and metal complex to exclude the metal–olefin π -bonding term

from the consideration. The calculations were carried out using the Gaussian98 program.⁶⁰

Results

Here we will briefly describe the calculated geometries and relative energies of stationary points of the potential energy surfaces corresponding to the reductive elimination (Scheme 1) from Pt^{IV} , Pt^{II} , Pd^{IV} , Pd^{II} , Ru^{II} , Os^{II} , Rh^{III} , and Ir^{III} derivatives. We will outline the main trends in the geometries and energetics, while the discussions of the possible reasons for these trends will be given in the Discussion. Each studied reaction will be referred as a separate numbered entry in the tables and text, while Init, TS, π -Comp, and Prod notations will be used to mark initial reactant, transition states, π -complexes, and products, respectively (Scheme 1). For the reaction of the complex $[\text{Pt}(\text{CH}=\text{CH}_2)_2\text{X}_4]^{2-}$ (**1**), we have studied two distinct paths leading to *s*-cis and *s*-trans products, and the stationary points corresponding to the *s*-cis path will be referred as **1A_Init**, **1A_TS**, **1A_π-Comp**, and **1A_Prod**, respectively.

A. Reductive Elimination from Platinum Compounds. Pt^{IV} Halogen Complexes $[\text{Pt}(\text{CH}=\text{CH}_2)_2\text{X}_4]^{2-}$ ($X = \text{Cl}, \text{Br}, \text{I}$). In contrast to C–C reductive elimination of methyl groups, the reaction involving vinyl ligands may proceed via two different transition states. The origin of this difference comes from the geometry of the conjugated buta-1,3-diene unit being formed. It may possess either *s*-cis or *s*-trans configuration around the central single bond (Figure 1). Both transition states were located in the case of platinum(IV) chloride complexes (**1_TS** and **1A_TS**); the corresponding energies are given in Table 1, and selected optimized structural parameters are listed in Table 2. We note here that, at the present level of theory, the calculated relative energies of *s*-trans, *s*-gauche, and *s*-cis conformers are 0.0, 3.5, and 4.0 kcal/mol, respectively, in agreement with earlier findings.⁶¹

Reductive elimination through the *s*-trans pathway retains C_2 symmetry and has to overcome the activation barrier of 29.4 kcal/mol. On the other hand, initial complex (**1A_Init**) and transition states (**1A_TS**) for the *s*-cis pathway belong to the C_s point group and the activation energy is 4.9 kcal/mol higher than for the former (Table 1). In the latter process, the product buta-1,3-diene will be released in the *s*-gauche (C_2) form. Reductive elimination reactions are exothermic by 17.0 and 19.9 kcal/mol for *s*-cis and *s*-trans pathways, respectively (Table 1).

The energy difference between the initial bis- σ -vinyl complexes **1_Init** and **1A_Init** is only 0.6 kcal/mol with the former being more stable. The structures can be easily interconverted to each other via rotation of vinyl ligands around a Pt–C bond, which has been shown to proceed with small barrier of a few kilocalories per mole.¹³ Both transition states (**1_TS** and **1A_TS**) have a similar three-centered character with minor differences

(46) d-Polarization function exponent 0.266. According to ref 43.

(47) Cossi, M.; Barone, V.; Cammi, R.; Tomasi, J. *Chem. Phys. Lett.* **1996**, *255*, 327.

(48) Fortunelli, A.; Tomasi, J. *Chem. Phys. Lett.* **1994**, *231*, 34.

(49) Tomasi, J.; Persico, M. *Chem. Rev.* **1994**, *94*, 2027.

(50) Floris, F.; Tomasi, J. *J. Comput. Chem.* **1989**, *10*, 616.

(51) Pascual-Ahuir, J. L.; Silla, E.; Tomasi, J.; Bonaccorsi, R. *J. J. Comput. Chem.* **1987**, *8*, 778.

(52) Mieritus, S.; Tomasi, J. *J. Chem. Phys.* **1982**, *65*, 239.

(53) Mieritus, S.; Scrocco, E.; Tomasi, E. *J. Chem. Phys.* **1981**, *55*, 117.

(54) Barone, V.; Cossi, M.; Tomasi, J. *J. Chem. Phys.* **1997**, *107*, 3210.

(55) Pomeli, C. S.; Tomasi, J.; Sola, M. *Organometallics* **1998**, *17*, 3164.

(56) Cacelli, I.; Ferretti, A. *J. Chem. Phys.* **1998**, *109*, 8583.

(57) Creve, S.; Oevering, H.; Coussens, B. B. *Organometallics* **1999**, *18*, 1907.

(58) Bernardi, F.; Bottoni, A.; Miscone, G. P. *Organometallics* **1998**, *17*, 16.

(59) Wiberg, K. B.; Rablen, P. R. *J. Am. Chem. Soc.* **1993**, *115*, 9234.

(60) Frisch, M. J.; Trucks, G. W.; Schlegel, H. B.; Scuseria, G. E.; Robb, M. A.; Cheeseman, J. R.; Zakrzewski, V. G.; Montgomery, J. A., Jr.; Stratmann, R. E.; Burant, J. C.; Dapprich, S.; Millam, J. M.; Daniels, A. D.; Kudin, K. N.; Strain, M. C.; Farkas, O.; Tomasi, J.; Barone, V.; Cossi, M.; Cammi, R.; Mennucci, B.; Pomelli, C.; Adamo, C.; Clifford, S.; Ochterski, J.; Petersson, G. A.; Ayala, P. Y.; Cui, Q.; Morokuma, K.; Malick, D. K.; Rabuck, A. D.; Raghavachari, K.; Foresman, J. B.; Cioslowski, J.; Ortiz, J. V.; Baboul, A. G.; Stefanov, B. B.; Liu, G.; Liashenko, A.; Piskorz, P.; Komaromi, I.; Gomperts, R.; Martin, R. L.; Fox, D. J.; Keith, T.; Al-Laham, M. A.; Peng, C. Y.; Nanayakkara, A.; Gonzalez, C.; Challacombe, M.; Gill, P. M. W.; Johnson, B.; Chen, W.; Wong, M. W.; Andres, J. L.; Gonzalez, C.; Head-Gordon, M.; Replogle, E. S.; Pople, J. A. *Gaussian 98*, Gaussian, Inc., Pittsburgh, PA, 1998.

(61) Wiberg, K. B.; Rablen, P. R.; Marquez, M. *J. Am. Chem. Soc.* **1992**, *114*, 8654.

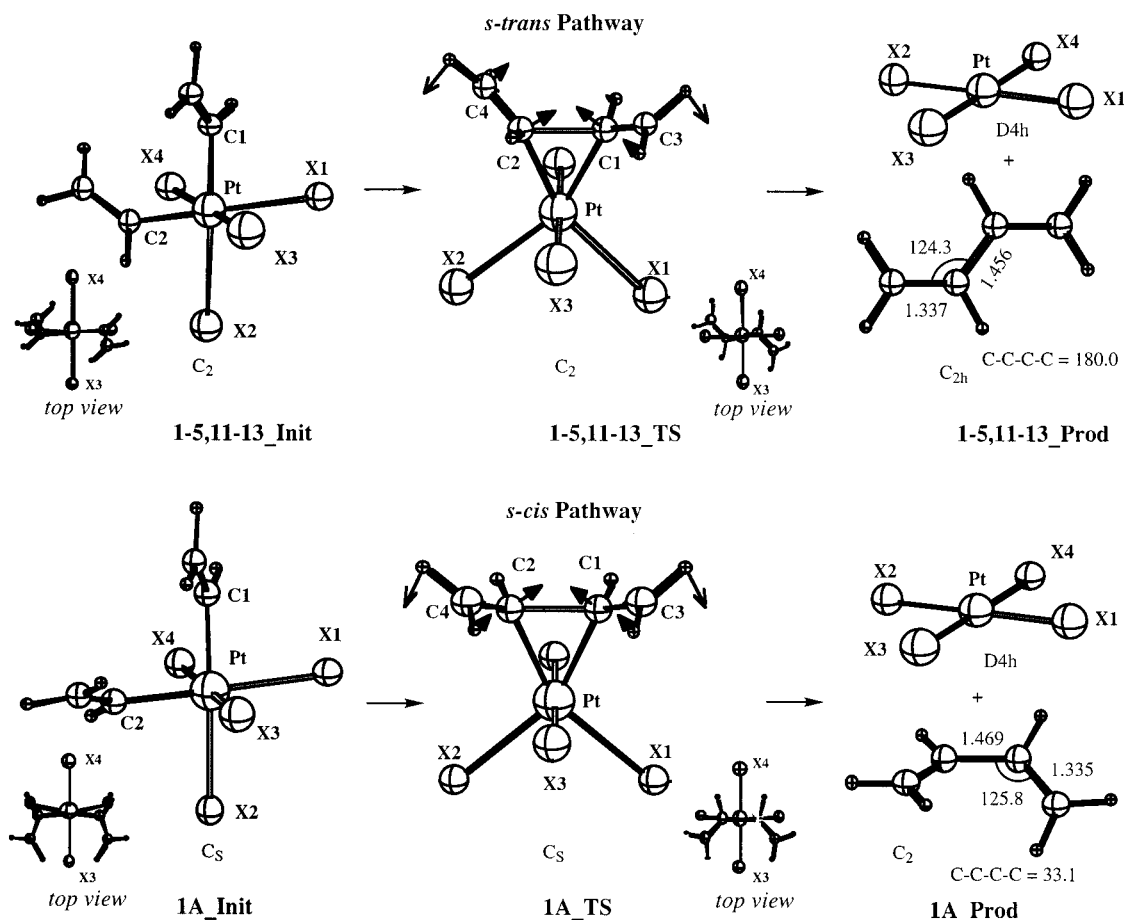


Figure 1. S-cis and s-trans reductive elimination pathways from octahedral complexes.

in geometry except for the conformation of the carbon skeleton (Table 2). The relative order of the transition states reflects the stability of corresponding buta-1,3-diene isomers in a free form. Thus, s-cis transition states are expected to lie higher in energy (see also ref 13 and the section Steric Effect Induced by Substituents on Vinyl Groups below) and we will continue the study following the s-trans pathway only.

To analyze possible origins of relative stability order, the deformation energies of the buta-1,3-diene and $PtCl_4^{2-}$ units were evaluated from the single point calculations at the corresponding transition-state geometries (**1_TS** and **1A_TS**). Both buta-1,3-diene and $PtCl_4^{2-}$ units are more stable by 0.8 and 0.1 kcal/mol, respectively, in the case of **1_TS** geometry (s-trans pathway). Thus, deformation energy (0.9 kcal/mol) accounts for only a small part of the energy differences between **1_TS** and **1A_TS** (4.9 kcal/mol), while the rest can be attributed to interaction energy contribution due to the earlier character of the former transition state.

Upon examination of the C–C reductive elimination reaction from a series of halogen complexes (Pt^{IV} : X = Cl, Br, I; Table 1), a clear trend is observed; the heavier the ligand, the smaller the activation barrier, and the larger the exothermicity of the process. Therefore, the easier reductive elimination reaction should be expected from iodide complexes of Pt^{IV} with the activation energy of only 25.0 kcal/mol and reaction energy of -30.3 kcal/mol. The changes in geometry are in line with the energies. In particular, the latest transition state is found for the chloride complex (**1_TS**) with the shortest C1–C2 distance

of 1.741 Å, which is increased to 1.785 and 1.829 Å for bromide (**2_TS**) and iodide (**3_TS**) derivatives, respectively (Table 2). The length of the Pt–C bond in initial compounds (**1_Init** to **3_Init**, Table 2) is increased upon going from X = Cl to X = I in agreement with the expected order of trans effect: $I > Br > Cl$, which is known to make the bond in trans position longer. The reactivity of the complexes in the C–C bond formation reaction increases in the same order.

Mixed Pt^{IV} Complexes $[Pt\{cis/trans-(CH=CH_2)_2(PH_3)_2\}Cl_2]$. Introducing phosphine ligands either in cis or trans position to σ -vinyl groups favors C–C bond formation (Table 1). However, in the case of trans substitution (**4**) the influence is much larger, $\Delta E^\ddagger = 18.5$ kcal/mol, compared to $\Delta E^\ddagger = 27.6$ kcal/mol for cis derivative **5** and $\Delta E^\ddagger = 29.4$ kcal/mol for the chloride complex **1**. It is found that lower activation barriers are accompanied by higher reaction exothermicities (cf. ΔE for **1**, **4**, and **5** in Table 1). Geometry changes follow the trends outlined earlier for the halogen complexes (Table 2).

Reactions of both **4** and **5** lead to the same products, $trans-[Pt(PH_3)_2Cl_2]$ and buta-1,3-diene. Therefore, the difference in reaction energies (ΔE) reflects the relative stability of initial bis- σ -vinyl derivatives; **5_Init** is thermodynamically more stable by 7.2 kcal/mol than **4_Init**. Very likely, destabilization of **4_Init** due to mutual trans orientation of vinyl and phosphine ligands is responsible for facilitating the reductive elimination process **4_Init** \rightarrow **4_TS** \rightarrow **4_Prod**.

Pt^{II} Halogen Complexes $[Pt(CH=CH_2)_2X_2]^{2-}$ (X = Cl, Br, I). C–C bond formation initiated from the square planar

Table 1. Activation (ΔE^\ddagger , ΔH^\ddagger , ΔG^\ddagger) and Reaction Energies (ΔE , ΔH , ΔG) of the C–C Reductive Elimination Stage in the Gas Phase and $\Delta G_{\text{aq}}^\ddagger$ and ΔG_{aq} in Water Solution (in kcal/mol)^a

no.	system ^b	ΔE^\ddagger	ΔE	ΔH^\ddagger	ΔH	ΔG^\ddagger	ΔG	$\Delta G_{\text{aq}}^\ddagger$	ΔG_{aq}
1	Pt(IV), X = Cl	29.4	−19.9	28.6	−19.4	29.2	−30.6	22.3	−44.4
1A	Pt(IV), X = Cl, s-cis ^c	34.3	−17.0	34.0	−16.0	33.2	−28.0		
2	Pt(IV), X = Br	27.2	−25.3	26.4	−24.8	26.5	−35.9	20.0	−45.4
3	Pt(IV), X = I	25.0	−30.3	24.2	−29.9	24.3	−41.4	20.2	−50.6
4	Pt(IV), X1, X2 = PH ₃ ; X3, X4 = Cl	18.5	−40.4	17.5	−39.9	18.0	−52.2	18.0	−55.3
5	Pt(IV), X1, X2 = Cl; X3, X4 = PH ₃	27.6	−33.2	26.5	−33.5	27.6	−46.6	22.0	−43.8
6	Pt(II), X = Cl	40.6	−3.7/26.1	39.1	−2.9/27.6	39.0	−3.0/17.9	23.9	−15.4/−18.3
7	Pt(II), X = Br	35.4	−8.3/20.6	34.2	−7.3/21.9	34.0	−7.5/12.6	20.3	−20.1/−19.0
8	Pt(II), X = I	31.2	−12.3/13.0	30.0	−11.3/14.3	29.9	−11.5/5.0	22.0	−20.2/−24.6
9	Pt(II), X = NH ₃	35.2	−8.5/0.9	33.7	−7.8/1.5	32.2	−9.3/−10.0	31.3	−11.5/−14.9
10	Pt(II), X = PH ₃	19.3	−27.4/−17.8	18.2	−26.4/−17.5	18.5	−26.9/−29.0	18.7	−26.5/−29.8
11	Pd(IV), X = Br	12.9	−51.3	12.5	−50.5	12.9	−61.2	8.2	−67.4
12	Pd(IV), X = I	11.4	−55.4	10.9	−54.6	11.3	−65.8	12.0	−72.8
13	Pd(IV), X1, X2 = PH ₃ ; X3, X4 = Cl	7.3	−57.4	6.6	−56.3	7.2	−67.4	7.9	−70.6
14	Pd(II), X = Cl	18.9	−22.2/2.3	17.8	−21.1/4.2	18.2	−21.2/−5.2	8.1	−31.1/−40.8
15	Pd(II), X = Br	15.0	−26.9/−4.8	14.0	−25.6/−3.1	14.2	−26.0/−12.2	4.7	−35.5/−39.7
16	Pd(II), X = I	11.9	−30.8/−12.0	11.0	−29.5/−10.4	11.0	−29.9/−19.4	4.5	−37.2/−44.4
17	Pd(II), X = NH ₃	15.3	−25.7/−15.4	14.3	−24.8/−14.7	13.6	−26.0/−25.5	13.6	−26.8/−29.5
18	Pd(II), X = PH ₃	6.8	−42.3/−33.8	5.9	−41.0/−33.3	6.1	−42.1/−44.4	7.8	−42.0/−44.6
19	[Rh ^{III} (CH=CH ₂) ₂ (PH ₃) ₃ Cl]	17.8	−29.1	16.8	−28.8	18.2	−41.0	18.7	−42.3
20	[Ir ^{III} (CH=CH ₂) ₂ (PH ₃) ₃ Cl]	28.5	−13.8	27.3	−13.7	28.4	−26.4	29.2	−28.0
21	[Ru ^{III} (CH=CH ₂) ₂ (PH ₃) ₃]	28.1	−44.8/23.2	27.6	−42.8/21.9	29.7	−39.0/13.0	27.3	−40.1/12.9
22	[Os ^{III} (CH=CH ₂) ₂ (PH ₃) ₃]	34.1	−42.2/35.0	33.5	−40.1/34.2	35.5	−36.2/23.4	33.8	−36.7/23.7

^a $\Delta E^\ddagger = E(\text{TS}) - E(\text{Init})$; for M^{IV} complexes: $\Delta E = E(\text{Prod}) - E(\text{Init})$; for M^{II} complexes: $\Delta E = E(\pi\text{-Comp}) - E(\text{Init})$, while the values after / correspond to $\Delta E = E(\text{Prod}) - E(\text{Init})$. The same is applicable also for enthalpies and free energies. For stationary point structures, see Figures 1–3. ^b Two vinyl ligands are cis to each other, X1 and X2 are trans to vinyl ligands, and X3 and X4 are trans to each other. ^c Reductive elimination through the s-cis pathway (see Figure 1); all the other calculations were done for the s-trans pathway.

bis- σ -vinyl complexes (**6**, **7**, **8**) also proceeds through the three-centered transition state (Figure 2). Upon metal–carbon σ -bond breakage and reductive elimination, the coordination vacancy becomes available at the metal center and a π -complex of buta-1,3-diene is formed. Double bond coordination ($\eta^2\text{-C}=\text{C}$) to the metal atom is preferred in this case, while the structure with central C–C bond coordination has an imaginary frequency corresponding to $\eta^2\text{-C}=\text{C} \rightarrow \eta^2\text{-C}=\text{C}$ rearrangement.⁶²

The same trend as noted above for Pt^{IV} is observed for the series of Pt^{II} complexes (**6**–**8**, Table 1); heavier halogen ligands make C–C bond formation easier by decreasing the activation energy and favoring the process thermodynamically. Geometry changes (Table 3) are consistent with the energetics; the lower the activation barrier height, the earlier the transition state: C1–C2 = 1.666 (for **6**_TS, X = Cl), 1.700 (for **7**_TS, X = Br), and 1.733 Å (for **8**_TS, X = I). However, comparing the C–C reductive elimination reaction from Pt^{II} (**6**–**8**, Table 1) complexes with those of Pt^{IV} (**1**–**3**, Table 1) complexes, one can deduce a clear preference of the higher oxidation state. For the Pt^{IV} derivatives, the activation barriers are lower by 11.2–6.2 kcal/mol and the processes are more exothermic by 16.2–18.0 kcal/mol than the corresponding Pt^{II} species.

Another interesting feature of the Pt^{II} system deserves special notice. Upon dissociation of the π -complex, an unusual Pt⁰ species, PtX₂²⁻, is formed. However, the energies of these stationary points are rather high, suggesting the compounds are unlikely to be sufficiently stable. Formation of analogous zerovalent anionic complexes of Pd⁰ was detected by experiment.⁶³

Pt^{II} Complexes with Amine and Phosphine Ligands [Pt(CH=CH₂)₂X₂] (X = NH₃, PH₃). The energetics of C–C bond formation reaction starting from the amine complex **9** ($\Delta E^\ddagger = 35.2$ kcal/mol and $\Delta E = -8.5$ kcal/mol) are similar to those for the bromide derivatives ($\Delta E^\ddagger = 35.4$ kcal/mol and $\Delta E = -8.3$ kcal/mol, Table 1).

However, reductive elimination reaction from phosphine complex **10** is much easier with an activation energy of only 19.3 kcal/mol and reaction exothermicity of −27.4 kcal/mol (Table 1). This barrier is only slightly higher than that for the corresponding Pt^{IV} phosphine complex (**4**, Table 1). In addition, Pt(PH₃)₂ can be considered as a rather stable product in contrast to Pt(NH₃)₂ and PtX₂²⁻ (X = Cl, Br, I). The finding is consistent with the experimental experience that phosphine is often added to reaction mixtures to keep catalyst from decomposition so that the process can take place under homogeneous conditions.^{1,9,21,22} Obviously, phosphine derivatives are the best candidates for the reductive elimination process among the Pt^{II} complexes studied in the preset work.

B. Reductive Elimination from Palladium Compounds. Pd^{IV} Halogen Complexes [Pd(CH=CH₂)₂X₄]²⁻ (X = Cl, Br, I). In this case, C–C bond formation takes place rather easily with very low barriers of 12.9 and 11.4 kcal/mol for **11** (X = Br) and **12** (X = I), respectively (Table 1). These are ~14 kcal/mol lower than for the corresponding Pt^{IV} complexes, while the exothermicity of the reactions is increased by as much as 26 kcal/mol. The high exothermicity suggests very early transition state structures; in fact as seen in Table 2, for instance, the forming C–C bond is long, 2.038 Å, at **12**_TS for X = I. The results in Table 1 show that reductive elimination from Pd^{IV} complexes would proceed most easily among the M^{II} and M^{IV} halogen derivatives (M = Pt, Pd). It should be noted here

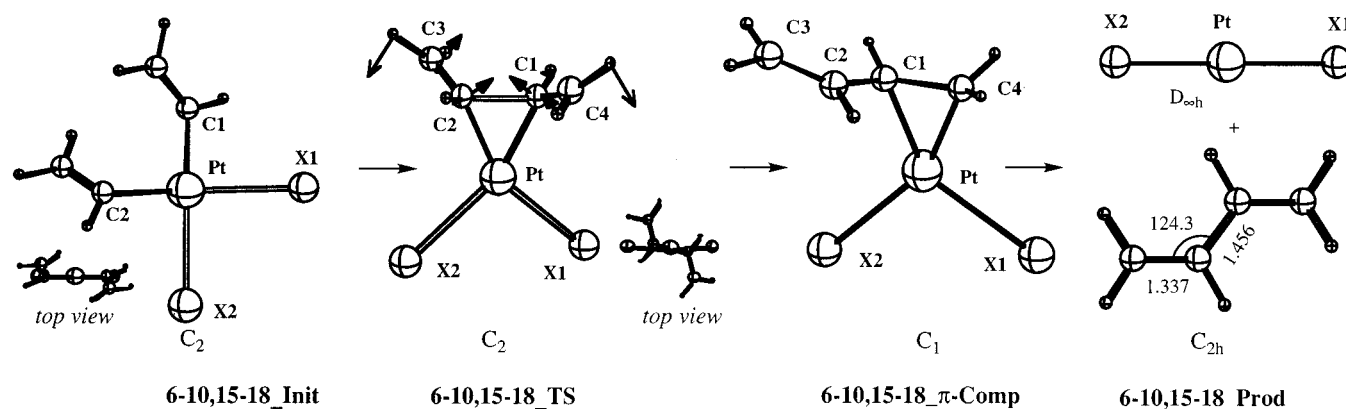
(62) See Figure S1 in Supporting Information.

(63) (a) Amatore, C.; Azzabi, M.; Jutand, A. *J. Am. Chem. Soc.* **1991**, *113*, 8375. (b) Negishi, E.; Takahashi, T.; Akiyoshi, K. *J. Chem. Soc. Chem. Commun.* **1986**, 1338.

Table 2. Selected Optimized Geometry Parameters for Pt^{IV} and Pd^{IV} Complexes (in Å and deg)^a

no., ligands	structure	M–C1	M–X1	M–X3	C1–C2	C1–M–X1	C1–M–X3	C1–M–C2
1 , X1–X4 = Cl	Init	2.022	2.597	2.459		85.0	90.9	95.2
	TS ^b Prod	2.126	2.613 2.455	2.461	1.741	107.6	86.2	48.4
1A , X1–X4 = Cl (s-cis)	Init	2.028	2.591	2.474		85.4	91.7 ^c	93.6
	TS ^b Prod	2.142	2.624 2.455	2.458	1.749	106.8	92.7 ^c	48.2
2 (11) , X1–X4 = Br	Init	2.030	2.771	2.594		85.4	91.1	94.8
	TS ^b	(2.032) 2.124 (2.091)	(2.774) 2.783 (2.783)	(2.584) 2.595 (2.585)		(84.8) 107.4 (102.5)	(85.4) 86.9 (87.2)	(95.0) 49.7 (56.7)
	Prod		2.585 (2.580)					
3 (12) , X1–X4 = I	Init	2.043	2.979	2.786		86.0	91.1	94.3
	TS ^b	(2.045) 2.130 (2.097)	(2.996) 2.983 (3.002)	(2.780) 2.789 (2.793)	1.829 (2.038)	(85.7) 106.0 (101.3)	(85.9) 87.7 (88.3)	(94.3) 50.8 (58.2)
	Prod		2.764 (2.767)					
4 (13) , X1, X2 = PH ₃ , X3, X4 = Cl	Init	2.070	2.476	2.451		87.0	94.0	86.6
	TS ^b	(2.057) 2.137 (2.097)	(2.522) 2.474 (2.544)	(2.422) 2.444 (2.410)	1.867 (2.045)	(88.6) 104.1 (102.4)	(94.5) 88.8 (89.1)	(85.1) 51.8 (58.4)
	Prod		2.314 (2.325)	2.422 (2.385)				
5 , X1, X2 = Cl, X3, X4 = PH ₃	Init	2.062	2.543	2.334		86.2	92.4	95.4
	TS ^b Prod	2.130	2.576 2.422	2.328 2.314	1.846	108.0	98.2	51.4 T

^a Values for M = Pd^{IV} are given in parentheses (see Figure 1 for structures). ^b Imaginary frequencies (in cm⁻¹): **1**_TS 448.5i, **1A**_TS 491.1i, **2**_TS 462.2i, **3**_TS 468.2i, **4**_TS 456.8i, **5**_TS 462.9i, **11**_TS 415.4i, **12**_TS 386.5i, and **13**_TS 394.5i. ^c C1–Pt–X4 = 86.4 and 86.1 for Init and TS, respectively.

**Figure 2.** S-trans reductive elimination pathway from square planar complexes.

that we were not able to locate the transition state for X = Cl; during geometry optimization two chloride ligands tend to dissociate, resulting in a structure similar to **14**_TS (see below).

Mixed Pd^{IV} Complex [Pd{trans-(CH=CH₂)₂(PH₃)₂}Cl₂]. We excluded from consideration the complexes with PH₃ ligands located cis to σ -bonded carbon atoms, since this type of Pt^{IV} derivative (**5**, Table 1) showed a very small effect of PH₃ on reaction energetics. Previous Pt^{IV}/Pt^{II} results (**4** and **10**, Table 1) suggest that phosphines trans to carbons should significantly facilitate the reductive elimination process. This trend seems

to be rather general and applicable to Pd^{IV} complexes as well; the corresponding Pd^{IV} complex **13** with phosphines trans to carbons has a low activation barrier for C–C bond formation of only 7.3 kcal/mol. In fact, this is the smallest activation energy found for all the M^{IV} complexes in the present work.

Pd^{II} Halogen Complexes [Pd(CH=CH₂)₂X₂]²⁻ (X = Cl, Br, I). Within the series of Pd^{II} halogen complexes **14** (X = Cl), **15** (X = Br), and **16** (X = I), the expected trends in the energies and geometry changes are again found; the heavier the halogen, the smaller the activation energy and earlier the

Table 3. Selected Optimized Geometry Parameters for Pt^{II} and Pd^{II} Complexes (in Å and deg)^a

no., ligands	structure	M–C1	M–X2	C1–C2	C2–C3	C1–C4	M–C4	C1–M–X1	C1–M–C2	X1–M–X2	
6 (14), X1, X2 = Cl	Init	1.984	2.613					86.4	95.0	92.3	
		(1.994)	(2.599)					(86.5)	(92.9)	(94.0)	
	TS ^b	2.066 (2.036)	2.638 (2.626)	–	1.666 (1.844)	–	–	–	107.5 (102.7)	47.5 (53.8)	97.8 (101.6)
	π -Comp	2.105 (2.173)	2.613 (2.614)	2.623 (2.618)	1.458 (1.447)	1.350 (1.354)	1.469 (1.439)	2.033 (2.041)	114.9 ^c (114.5 ^c)	41.5 ^d (39.8 ^d)	95.4 (103.5)
	Prod		2.470 (2.491)								
7 (15), X, X2 = Br	Init	1.984	2.811	–	–	–	–	86.5	94.2	92.8	
		(1.992)	(2.819)					(86.8)	(92.0)	(94.5)	
	TS ^b	2.060 (2.030)	2.826 (2.853)	–	1.700 (1.900)	–	–	–	107.2 (101.4)	48.7 (55.8)	97.9 (103.4)
	π -Comp	2.107 (2.175)	2.804 (2.873)	2.800 (2.816)	1.461 (1.451)	1.347 (1.350)	1.460 (1.429)	2.038 (2.055)	115.1 ^c (115.3 ^c)	41.2 ^d (39.4 ^d)	97.2 (106.6)
	Prod		2.585 (2.646)								
8 (16), X1, X2 = I	Init	1.988	3.017					86.8	93.1	93.2	
		(1.994)	(3.039)					(87.1)	(91.0)	(94.8)	
	TS ^b	2.068 (2.031)	2.983 (3.037)		1.733 (1.937)				105.7 (100.3)	49.7 (57.0)	100.5 (105.5)
	π -Comp	2.118 (2.185)	2.964 (3.042)	2.957 (2.977)	1.461 (1.452)	1.346 (1.348)	1.455 (1.424)	2.048 (2.070)	114.0 ^c (114.1 ^c)	40.8 ^d (39.0 ^d)	100.5 (109.2)
	Prod		2.717 (2.771)								
9 (17), X1, X2 = NH ₃	Init	2.000	2.249					87.0	90.3	95.7	
		(2.002)	(2.250)					(88.2)	(87.7)	(95.9)	
	TS ^b	2.067 (2.033)	2.329 (2.319)		1.669 (1.882)				112.1 (105.2)	47.6 (55.1)	88.1 (94.4)
	π -Comp	2.086 (2.112)	2.310 (2.299)	2.296 (2.331)	1.455 (1.464)	1.339 (1.343)	1.472 (1.425)	2.058 (2.095)	113.4 ^c (107.5 ^c)	41.1 ^c (39.6 ^d)	88.9 (97.2)
	Prod		2.072 (2.106)								
10 (18), X1, X2 = PH ₃	Init	2.062	2.357					86.7	84.7	101.9	
		(2.052)	(2.380)					(86.1)	(82.9)	(104.9)	
	TS ^b	2.104 (2.071)	2.349 (2.395)		1.864 (2.022)				102.0 (97.5)	52.1 (58.4)	104.2 (106.5)
	π -Comp	2.188 (2.242)	2.326 (2.344)	2.317 (2.355)	1.469 (1.464)	1.339 (1.339)	1.428 (1.398)	2.149 (2.196)	105.6 ^c (104.6 ^c)	38.4 ^d (36.7 ^d)	108.7 (112.8)
	Prod		2.261 (2.291)								

^a Values for M = Pd^{II} are given in parentheses (see Figure 2 for structures). ^b Imaginary frequencies (in cm⁻¹): **6**_TS 477.7i, **7**_TS 480.9i, **8**_TS 484.4i, **9**_TS 369.2i, **10**_TS 450.2i, **14**_TS 461.2i, **15**_TS 443.7i, **16**_TS 426.9i, **17**_TS 433.3i, and **18**_TS 378.6i. ^c C1–Pt–X2 in the case of π -Comp. ^d C4–Pt–C1 in the case of π -Comp.

transition state, with longer C1–C2 bond and larger C1–Pt–C2 angle (Table 3, Figure 2). The smallest barrier is calculated for the iodide complex, $\Delta E^\ddagger = 11.9$ kcal/mol, and the largest, 18.9 kcal/mol, for chloride, with bromide between, 15.0 kcal/mol. An increase in activation energies is accompanied by a decrease in exothermicity (Table 1). As discussed earlier for the corresponding platinum compounds, reductive elimination reaction from Pd^{II} halogen complexes also gives anionic Pd⁰ species.⁶³

Pd^{II} Complexes with Nitrogen and Phosphine Ligands [Pd(CH=CH₂)₂X₂] (X = NH₃, PH₃). Very similar geometries for both initial compound and transition state are found for the complexes with X = NH₃ and X = Br (**17** and **15** in Table 3). The activation and reaction energies are also similar: $\Delta E^\ddagger = 15.0$ and 15.3 kcal/mol and $\Delta E = -26.9$ and -25.7 kcal/mol for X = Br and X = NH₃, respectively (Table 1). Thus, both complexes would show a similar reactivity in the reductive elimination process. However, the stability of [Pd⁰Br₂]²⁻ and

[Pd⁰(NH₃)₂] relative to the corresponding π -complex differs significantly, the former being ~ 11 kcal/mol less stable than the latter.

For the Pd^{II} phosphine complex **18**, vinyl–vinyl coupling reaction is very easy, with the barrier only 6.8 kcal/mol, the smallest barrier reported in this article. The **18**_TS is a very early transition state with the forming bond of C1–C2 = 2.022 Å and C1–Pd–C2 angle of 58.4° (Table 3).

C. Reductive Elimination from Rh^{III}, Ir^{III}, Ru^{II}, and Os^{II} Complexes. We extended the study of C–C reductive elimination reactions to other members of late transition metals in order to find possible alternatives to Pd/Pt complexes for catalytic coupling reactions. The calculations were performed only for the corresponding phosphine complexes, for which experimental precedents for the reaction were reported.^{18–20} In the case of rhodium and iridium derivatives, an extra σ -bonded ligand has to be added to maintain the correct oxidation state, because Rh^{II} and Ir^{II} compounds are rarely known.⁶⁴ The chloride has been

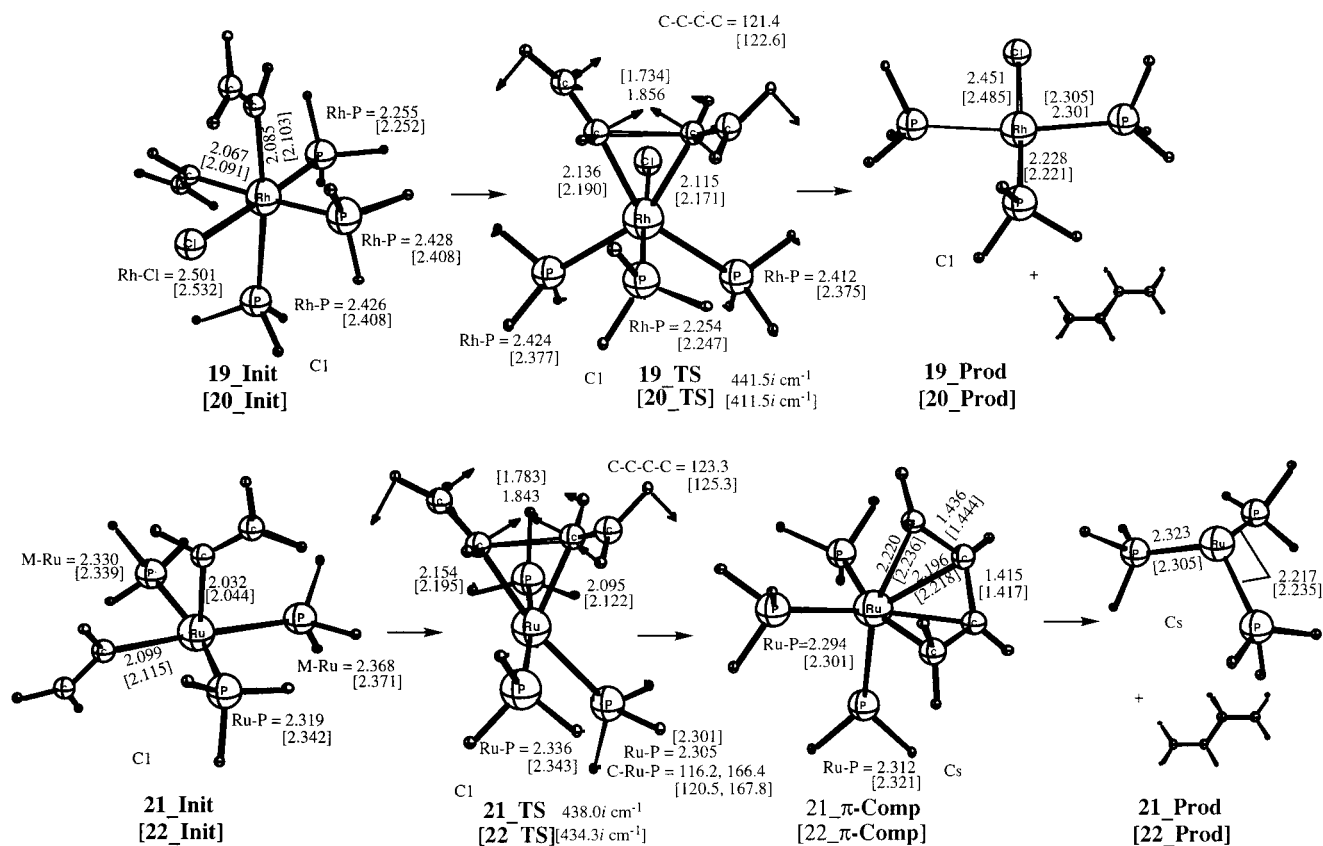


Figure 3. Optimized geometry structures for Rh^{III} and Ir^{III} (top) and Ru^{II} and Os^{II} (bottom) reductive elimination reactions. Parameters for Ir^{III} and Os^{II} derivatives are given in brackets.

chosen for this purpose. Thus, the model compounds studied are **19** [Rh^{III}(CH=CH₂)₂(PH₃)₃Cl], **20** [Ir^{III}(CH=CH₂)₂(PH₃)₃Cl], **21** [Ru^{II}(CH=CH₂)₂(PH₃)₃], and **22** [Os^{II}(CH=CH₂)₂(PH₃)₃].

As in the previous cases (Figure 1 and Figure 2), vinyl–vinyl coupling for these compounds also occurs through the three-centered transition states (Figure 3). The lengths of the forming C–C bonds at the transition state for Ir^{III} and Os^{II} compounds (1.734 and 1.783 Å) are considerably shorter than for Rh^{III} and Ru^{II} (1.856 and 1.843 Å) analogues. The Wilkinson-type **19_Prod** and its iridium analogue **20_Prod** are formed as final products for the first two reactions. In agreement with the experimental studies, initial Ru^{II} and Os^{II} complexes have square-pyramidal structure,¹⁹ while the products are η⁴-coordinated π-complexes, **21_π-Comp** and **22_π-Comp**.^{19,20} It is interesting to note that in **21_TS** and **22_TS** the axial PH₃ ligand does not occupy a symmetrical position with respect to the carbon atoms but rather is located trans to one of them (Figure 3). The smallest activation barrier among these four compounds is found for Rh^{III} **19** (17.8 kcal/mol), while those for the other complexes are considerably higher (28.1–34.1 kcal/mol). To summarize, the present calculations show that Rh^{III}-based complexes can be considered as possible catalysts for vinyl–vinyl reductive elimination, while Ir^{III}, Ru^{II}, and Os^{II} analogues are likely to be less active. Once, again, our calculations shown that the second-row metals have lower barriers as well as higher exothermicities than the third-row metals within each subgroup (Table 1): Rh^{III} > Ir^{III} and Ru^{II} > Os^{II}.

Discussion

Thus, our calculations, in agreement with the available experiments, have demonstrated that the reactivity of the [M(CH=CH₂)₂X_n] complexes (for M = Pd and Pt) in C–C bond formation depends on the nature of the ligand X and decreases in the order X = PH₃ > I > Br, NH₃ > Cl for both M^{IV} and M^{II} oxidation states. In all the cases, phosphine ligands decrease the activation barriers and increase the exothermicity of the reaction. The present results also show that, without exception, all the second-row metals (Ru, Rh, Pd) show lower barriers and higher exothermicities than the corresponding third-row metals (Os, Ir and Pt) within each subgroup (Table 1), i.e., the reactivity of the studied complexes decreases via Pd^{II} > Pt^{II}, Pd^{IV} > Pt^{IV}, Rh^{III} > Ir^{III}, and Ru^{II} > Os^{II}. The complexes of Pt^{IV} are more reactive than corresponding complexes of Pt^{II}. Similar results have been obtained for Pd complexes, while for them this effect is less pronounced. Considering the most reactive phosphine complexes, the following overall relative reactivity order in vinyl–vinyl coupling reaction may be suggested for these metals: Pd^{IV}, Pd^{II} > Pt^{IV}, Pt^{II}. Thus, Pd complexes are suggested to be the most reactive for this reaction.

In this section, the major factors controlling the reactivity of the transition metal complexes studied here will be discussed. At first, the electronic effects arising from the metal atoms M and ligands X will be analyzed, followed by consideration of closely related topics of metal–carbon bond strengths and ligand trans effect (trans influence). Next, we will discuss the steric effects arising both from the ligands X and from the substituents on the vinyl groups. Finally, we will analyze the asymmetric nature of vinyl–vinyl coupling followed by comparison with

(64) Cotton, S. A. *Chemistry of Precious Metals*; Blackie Academic and Professional (Chapman & Hall): London, 1997.

Table 4. Promotion and Averaged Reaction Energies (in kcal/mol) for C–C Reductive Elimination Reactions from Platinum and Palladium Complexes^{a,b}

reaction	atomic energy difference ^c		$\Delta E_{\text{averaged}}$			
	Pd	Pt	X = Cl, Br, I		X = PH ₃ , NH ₃ ^d	
			Pd	Pt	Pd	Pt
M ^{IV} → M ^{II} (s ² d ⁸ → s ¹ d ⁹)	-56.0	-14.8	-53.4 (11, 12)	-27.8 (2, 3)	-57.4	-40.4
M ^{II} → M ⁰ (s ¹ d ⁹ → d ¹⁰)	-21.9	11.1	-4.8 (14–16)	19.9 (6–8)	-33.8 [-15.4]	-17.8 [0.9]

^a The compounds used for averaging are given in parentheses (see Table 1 for energies and Figures 1 and 2 for structures). ^b For Pt^{II} and Pd^{II}, ΔE with respect to the final products (MX₂ + diene), rather than to π -complexes is used (see captions to Table 1). ^c Experimentally determined; see text for details. ^d Values for X = NH₃ are given in brackets.

the well-known C_{sp3}–C_{sp3} elimination reaction. The study of the solvent effect will also be discussed.

A. Reaction Energetics in Terms of Electronic Configuration of the Metal Atoms and Electronic Nature of the Ligand X. As was pointed out earlier,^{30,65} the change in the degree of oxidation of metal atoms during the oxidative addition/reductive elimination reactions could be described in terms of the promotion of electronic configuration of metal atoms. In the M⁰, M^{II}, and M^{IV} complexes, both Pt and Pd atoms possess, d¹⁰, s¹d⁹, and s²d⁸ electronic configurations, respectively.⁶⁶ In M⁰, no covalent bonds are possible, since all five d orbitals are doubly occupied. In contrast, M^{II} and M^{IV} atoms can make two and four covalent bonds, respectively, through the hybrid s and d orbitals. The energy differences between the lower-lying electronic configurations of Pd and Pt atoms and the calculated average reaction energies for C–C reductive elimination reactions of the Pd/Pt complexes are given in Table 4.

As seen from Table 4 and Table 1, the concept of lower lying electronic configurations provides reliable qualitative description of the systems studied. In particular, (i) M^{IV} → M^{II} reductive elimination is always more exothermic than M^{II} → M⁰, which is consistent with the calculated s²d⁸ → s¹d⁹ and s¹d⁹ → d¹⁰ promotion energies, and (ii) both Pd^{IV} → Pd^{II} and Pd^{II} → Pd⁰ processes are more exothermic compared to Pt^{IV} → Pt^{II} and Pt^{II} → Pt⁰, which is again agrees with the calculated s²d⁸ → s¹d⁹ and s¹d⁹ → d¹⁰ promotion energies of Pd and Pt atoms. In agreement with the Hammond postulate, (i) the activation energies are lower when the reaction starts from M^{IV} derivatives than from M^{II}, and (ii) C–C bond formation involving palladium complexes requires significantly smaller barriers than with platinum.

Although the energetics of reductive elimination from platinum and palladium complexes without extra ligands (such as PH₃ and NH₃) is quantitatively correlated with the atomic energy differences,^{30,33} in the case with extra ligands, only a qualitative agreement is observed. The main reason for this difference comes from the fact that ligands, which are not directly involved in the reaction, stabilize electronic states in a different manner. Considering reductive elimination transformation M^{II} → M⁰ and

using halogen ligands as reference point, we define the stabilization energy for NH₃ ($\Delta\Delta E_1$) and PH₃ ($\Delta\Delta E_2$) ligands as follows:

$$\Delta\Delta E_1 = \Delta E(\text{halogens}) - \Delta E(\text{NH}_3) \quad \text{and}$$

$$\Delta\Delta E_2 = \Delta E(\text{halogens}) - \Delta E(\text{PH}_3)$$

According to Table 4, $\Delta\Delta E_1 = 10.6$ and 19.0 kcal/mol for M = Pd^{II} and Pt^{II}, respectively, and $\Delta\Delta E_2 = 29.0$ and 37.7 kcal/mol for M = Pd^{II} and Pt^{II}, respectively. In both cases, Pt complexes are stabilized more by almost the same value, $\Delta\Delta E_1(\text{Pt}) - \Delta\Delta E_1(\text{Pd}) = 8.4$ kcal/mol and $\Delta\Delta E_2(\text{Pt}) - \Delta\Delta E_2(\text{Pd}) = 8.7$ kcal/mol. In addition, the degree of stabilization by PH₃ ligand as compared to NH₃ ($\Delta\Delta E_2 - \Delta\Delta E_1$) is also very similar, 18.4 kcal/mol for M = Pd^{II} and 18.7 kcal/mol for M = Pt^{II}. Concerning the M^{IV} → M^{II} transformation, the influence of PH₃ seems to be much smaller, $\Delta\Delta E_2 = 4.0$ and 12.6 kcal/mol for M = Pd^{IV} and Pt^{IV}, respectively. However, the difference in stabilization between two metals, $\Delta\Delta E_2(\text{Pt}) - \Delta\Delta E_2(\text{Pd}) = 8.6$ kcal/mol, is similar to the M^{II} case.

The above discussion clearly indicates systematic ligand effects in the studied system, which can be summarized as follows. (i) PH₃ ligand stabilizes electronic states that have more electrons on d shells, i.e., d¹⁰ over s¹d⁹ and s¹d⁹ over s²d⁸; (ii) the degree of stabilization decreases in the order PH₃ > NH₃ > halogens; and (iii) platinum-based compounds are more sensitive to the stabilization effect than the corresponding palladium complexes. It should be noted that a similar qualitative electronic stabilization effect was observed in B–B oxidative addition reactions to zerovalent platinum and palladium phosphine complexes.⁶⁵

Similar considerations are also applicable for the reductive elimination reactions for the other platinum group metals. Our calculations on reductive elimination reactions have shown an energetic preference of Rh^{III} compounds to Ir^{III}, Ru^{II}, and Os^{II} compounds. The fact can be rationalized by taking into account that the only exothermic promotion energy of -37.6 kcal/mol^{66a} is expected for s²d⁷ → s¹d⁸ (Rh^{III} → Rh^I). In contrast, s²d⁷ → s¹d⁸ (Ir^{III} → Ir^I) and s¹d⁷ → d⁸ (Ru^{II} → Ru⁰) are endothermic by 25.1 and 9.2 kcal/mol, respectively.^{66a}

B. Metal–Carbon Bond Dissociation Energies. The calculated M–(CH=CH₂) bond dissociation energies for bis- σ -vinyl derivatives are listed in Table 5. In most cases, corresponding experimental values are not available; therefore, M–CH₃ bond strengths will be used for comparison. In discussing bond dissociation energies, we will consider (i) the ligand effect for M = Pt and Pd; (ii) the effect of oxidation state for Pt^{IV}/Pt^{II}, Pd^{IV}/Pd^{II}; and (iii) the metal effect for M = Pt^{II/IV}, Pd^{II/IV}, Rh^{III}, Ir^{III}, Ru^{II}, Os^{II}.

Ligand Effects. A very similar ligand effect is observed for platinum and palladium compounds in both oxidation states; bond strength decreases in the order Cl > Br > I > NH₃ > PH₃ (note, NH₃ for M^{II} only). These calculations are in agreement with the experimental measurements that relative Pt^{II}–CH₃ bond dissociation energy decreases in the order Cl > Br > I with the halogen ligands trans to the methyl group.⁶⁷

Effect of Oxidation State for Pd and Pt. The effect of oxidation state can clearly be resolved by comparing the respective halogen complexes; in both metals, (M = Pd, Pt) the M^{II}–(CH=CH₂) bond is by 23 kcal/mol stronger than M^{IV}–

(65) Cui, Q.; Musaev, D. G.; Morokuma, K. *Organometallics* **1998**, *17*, 742.

(66) (a) Moore, C. F. *Atomic Energy Levels*, NSRD-NBS.; U.S. Government Printing Office: Washington, DC, 1971; Vol. III. (b) Ground state for Pd atom is d¹⁰, while for Pt atom s¹d⁹. According to the above reference, experimentally determined relative energies averaged over spin–orbit components are (in kcal/mol) as follows: Pd d¹⁰(¹S) 0.0, s¹d⁹(³D) 21.9, s²d⁸(³F) 77.9; Pt s¹d⁹(³D) 0.0, d¹⁰(¹S) 11.1, s²d⁸(³F) 14.8. Supported with the relativistic ECP basis set, B3LYP very well reproduces the relative stability of these electronic states (see refs 13, 65, and 73).

Table 5. Calculated M–(CH=CH₂) and Experimental M–CH₃ Bond Dissociation Energies (in kcal/mol)

no.	complex ^a	BDE
1	[Pt ^{IV} (CH=CH ₂) ₂ Cl ₄] ²⁻	45.2
1A	[Pt ^{IV} (CH=CH ₂) ₂ Cl ₄] ²⁻	46.9 ^b
2	[Pt ^{IV} (CH=CH ₂) ₂ Br ₄] ²⁻	42.5
3	[Pt ^{IV} (CH=CH ₂) ₂ I ₄] ²⁻	39.9
4	[Pt ^{IV} {trans-(CH=CH ₂) ₂ (PH ₃) ₂ }Cl ₂] ²⁻	34.9
5	[Pt ^{IV} {cis-(CH=CH ₂) ₂ (PH ₃) ₂ }Cl ₂] ²⁻	38.1
	Pt ^{IV} –CH ₃ exp	32.4 ⁶⁹
6	[Pt ^{II} (CH=CH ₂) ₂ Cl ₂] ²⁻	68.7
7	[Pt ^{II} (CH=CH ₂) ₂ Br ₂] ²⁻	65.8
8	[Pt ^{II} (CH=CH ₂) ₂ I ₂] ²⁻	62.0
9	[Pt ^{II} (CH=CH ₂) ₂ (NH ₃) ₂]	55.6
10	[Pt ^{II} (CH=CH ₂) ₂ (PH ₃) ₂]	46.1
	Pt ^{II} –CH ₃ exp	61.7 ⁶⁸
11	[Pd ^{IV} (CH=CH ₂) ₂ Br ₄] ²⁻	29.6
12	[Pd ^{IV} (CH=CH ₂) ₂ I ₄] ²⁻	27.6
13	[Pd ^{IV} {trans-(CH=CH ₂) ₂ (PH ₃) ₂ }Cl ₂] ²⁻	26.7
14	[Pd ^{IV} (CH=CH ₂) ₂ Cl ₂] ²⁻	57.0
15	[Pd ^{IV} (CH=CH ₂) ₂ Br ₂] ²⁻	53.3
16	[Pd ^{IV} (CH=CH ₂) ₂ I ₂] ²⁻	49.7
17	[Pd ^{IV} (CH=CH ₂) ₂ (NH ₃) ₂]	47.5
18	[Pd ^{IV} (CH=CH ₂) ₂ (PH ₃) ₂]	38.2
	Pd ^{IV} –CH ₃ exp	43.4 ⁷⁰
19	[Rh ^{III} (CH=CH ₂) ₂ (PH ₃) ₃ Cl]	40.5
20	[Ir ^{III} (CH=CH ₂) ₂ (PH ₃) ₃ Cl]	48.0
21	[Ru ^{II} (CH=CH ₂) ₂ (PH ₃) ₃]	65.8
22	[Os ^{II} (CH=CH ₂) ₂ (PH ₃) ₃]	72.0

^a Corresponding Init compounds. ^b BDE for the initial bis- σ -vinyl compound corresponding to s-cis reductive elimination pathway.

(CH=CH₂). The results are consistent with the experimentally measured difference of 29.3 kcal/mol between Pt^{II}–CH₃ and Pt^{IV}–CH₃.^{68,69}

Metal Effects. Considering a pair of metals in each subgroup, the following effect of metal on M–(CH=CH₂) bond dissociation energies was obtained: Pt^{IV} > Pd^{IV}, Pt^{II} > Pd^{II}, Ir^{III} > Rh^{III}, Os^{II} > Ru^{II}. In short, heavier metals tend to form stronger bonds with σ -vinyl ligands. The experimentally observed difference of 18.3 kcal/mol between Pt^{II}–CH₃⁶⁸ and Pd^{IV}–CH₃⁷⁰ agrees with the 12–13 kcal/mol found in our work, despite the fact that experimental measurements were done for different complexes. Since, previously,⁷¹ the factors affecting the M–L bond energies upon going from the second-row transition metals to third-row metal have been discussed in more detail, here we will not repeat them.

Of course, one of the most interesting questions is whether the bond dissociation energy can be used to predict the relative activity of transition metal complexes in vinyl–vinyl coupling

(67) The mass spectral measurements actually determine the BDE of molecular ions rather than neutral complexes; however, it is generally accepted that these experiments provide the correct relative scale for the parent compounds (see also, a discussion): Morvillo, A.; Favero, G.; Turco, A. *J. Organomet. Chem.* **1983**, *243*, 111.

(68) Pt^{II}–CH₃ BDE averaged from 63.9 and 59.6 kcal/mol reported in: Al-Takhin, G.; Skinner, H. A.; Zaki, A. A. *J. Chem. Soc., Dalton Trans.* **1984**, 371.

(69) Several experimental values of Pt^{IV}–CH₃ bond dissociation energies are available: 30.9 and 32.8,^{69a} 31.6,^{23f} and 34.4 kcal/mol.^{23h} We will use the average value 32.4 kcal/mol of the experimentally determined bond dissociation energies. (a) Roy, S.; Puddephatt, R. J.; Scott, J. D. *J. Chem. Soc., Dalton Trans.* **1989**, 2121.

(70) A gas-phase value of 43.4 kcal/mol was obtained for Pd^{IV}–CH₃ from a guided ion beam mass spectrometry study.^{70a} The same method gives Pt^{IV}–CH₃ BDE of 61.6 kcal/mol,^{70b} which is in a good agreement with experimental value of 61.7 kcal/mol determined for Pt^{II}–CH₃.⁶⁸ (a) Chen, Y.-M.; Sievers, M. R.; Armentrout, P. B. *Int. J. Mass. Spectrom. Ion Processes* **1997**, *167/168*, 195. (b) Zhang, X.-G.; Liyanage, R.; Armentrout, P. B. *J. Am. Chem. Soc.* **2001**, *123*, 5563.

(71) See: Musaev, D. G.; Morokuma, K. *Organometallics* **1995**, *14*, 3327 and references therein.

reactions. For halogen complexes of both Pt and Pd in both low and high oxidation states, a very good correlation is observed; the larger the value of M–C bond dissociation energy, the higher the activation barrier. However, this is not the case if phosphine and nitrogen ligands are involved in comparison. Reductive elimination from complexes **5**_Init, [Pt^{IV}{cis-(CH=CH₂)₂(PH₃)₂}Cl₂]²⁻, and **2**_Init, [Pt^{IV}(CH=CH₂)₂Br₄]²⁻, is characterized with approximately the same activation energy (27.6 and 27.2 kcal/mol, respectively, Table 1), while the bond strength differs significantly (38.1 and 42.5 kcal/mol, respectively, Table 5). Similarly, the contradiction occurs while comparing bond dissociation energies and reaction barriers for amine and halogen ligands of Pt^{II} (cf. **9** and **6–8**, Tables 1 and 5) and Pd^{II} (cf. **17** and **14–16**, Tables 1 and 5). Therefore, metal–carbon bond strength could be used for estimating relative reactivity in the reductive elimination reaction only for ligands of similar nature (i.e., halogens). However, this single parameter fails to provide adequate prediction for a wide range of complexes.

Finally, it should be noted that the absolute values of the presented bond dissociation energies are subject to known limitations, although in such a cases the relative trends are believed to be reproduced correctly.⁷²

C. Trans Effect and Trans Influence in the Reactivity.

Both trans effect and trans influence of the ligands are widely applied to estimate and explain the reactivity of transition metal complexes. The former is defined as a kinetic factor related to transition state, while the latter describes the degree of bond strength weakening opposite to a particular ligand.⁶⁴ For the ligands investigated in the present work, trans effect and trans influence generally coincide in platinum complexes: PR₃ > I > Br > Cl > NH₃.⁶⁴ We will continue further discussion using the trans effect concept, keeping in mind that the same relative order should be expected if trans influence would be considered. Structural parameters exhibit some changes in agreement with the expected trans effect; particularly, in π -complexes the coordinated C=C bond becomes shorter, while the M–C bond becomes longer with an increasing trans effect (**6**_ π -Comp–**10**_ π -Comp, Table 3).

However, the concept fails to describe correctly energetic properties. Neither reaction exothermicities nor barrier heights follow the trend (Table 1). In addition, both relative orders of bond dissociation energy (Table 5) and π -complexation energy ($\Delta E = E_{\pi\text{-complex}} - E_{\text{Product}}$, for **6–10** in Table 1) disagree with the proposed trans effect. Therefore, our calculations show that, although widely implied and sometimes helpful in predicting structural changes, trans effect (trans influence) may not be reflected in energetic properties. As will be shown later, these rather complicated energetic dependencies are the result of existing electronic and steric factors in these systems, which do not follow the same trends.

D. Steric Effects from the Ligand X. Recently,^{32,73} it was shown that oxidative addition and reductive elimination processes may proceed through nonplanar transition states. Although electronic factors favor a planar structure due to maximum overlap with the preferred metal d orbital, steric factors cause deviation from planarity.³² Similar conclusions could be drawn from our calculations on the transition states

(72) Martinho, J. A.; Beauchamp, J. L. *Chem. Rev.* **1990**, *90*, 629.

(73) Cui, Q.; Musaev, D. G.; Morokuma, K. *Organometallics* **1997**, *16*, 1355.

Table 6. Angle between X–M–X and C–M–C Planes as a Function of X Ligand and Metal at the Transition State⁷⁴

M	X = Cl	X = Br	X = I	X = NH ₃	X = PH ₃
Pt ^{II}	8.9	13.8	16.9	2.9	6.4
Pd ^{II}	11.6	17.4	21.4	0.8	0.1
Pt ^{IV}	−7.0	−8.0	−8.6		−3.6 ^a
Pd ^{IV}		−6.8	−7.3		−2.5

^a Corresponds to **5**.

for reductive elimination for the present complexes. Indeed, our data indicate that these transition states are nonplanar; i.e., the forming C–C bond is tilted out of the X–M–X plane.⁷⁴ Moreover, the tilt angle increases by increasing the size of the halogen ligand X (see Table 6).

Based on the tilt angle presented in Table 6, the following order of the steric effects between X ligands can be suggested: I > Br > Cl > NH₃, PH₃. This is an expected trend. Indeed, here the steric effect includes electrostatic interactions and exchange (steric) repulsion with ligands X, and electrostatic interactions are expected to be larger in charged halogen complexes (X = Cl, Br, I) than the neutral ones (X = NH₃, PH₃). The tilt angle is found to be larger for Pd^{II} than Pt^{II}, since the former has an earlier transition state (Table 6).

Absolute values of the tilt angle exhibit the same trend for both M^{IV} and M^{II}. However, the values for M^{IV} are significantly smaller and have opposite sign. The differences between M^{IV} and M^{II} can be rationalized by taking into account that the former is an octahedral complex with two additional ligands in a perpendicular plane, which also interact with the vinyl groups. Repulsive interactions from ligands in octahedral complexes compensate each other, leading to smaller deviations from planar transition-state structure.⁷⁴ In agreement with geometrical trends, changing X from Cl to Br and from Br to I reduces the activation barriers by ~2 kcal/mol for Pt^{IV} and by ~5 kcal/mol for Pt^{II}. Also, in M^{IV} derivatives, carbon atoms of each vinyl ligand are located on the opposite sides of the X–M–X plane (in contrast to M^{II}), thus changing the sign of the tilt angle.⁷⁴

Thus, one may conclude that the reductive elimination process from initial complexes with square planar geometry may be more sensitive to the steric effects than from those with octahedral structure.

E. Steric Effect Induced by Substituents on Vinyl Groups.

Since the rotation around the carbon–carbon double bond in the vinyl group does not take place under normal experimental conditions, depending on the stereochemistry of the initial bis- σ -vinyl complex, (*E/E*)-, (*E/Z*)-, or (*Z/Z*)-dienes may be formed as final products.⁷⁵ The stereoselectivity problem is of vital importance in catalysis, and it deserves special attention.

A convenient model for this purpose is provided by the Pt^{IV}-catalyzed acetylene conversion reaction to (*E,E*)-1,4-diiodobuta-1,3-diene.¹² Here, in addition to the *E/E* pathway studied earlier,¹³ we investigate the *E/Z* and *Z/Z* pathways in order to find out factors controlling stereoselectivity of vinyl–vinyl coupling.

Optimized geometries for initial bis- σ -vinyl complexes, transition states, and products for *Z/E* and *Z/Z* coupling reactions

(74) See Figure S2 in Supporting Information.

(75) To avoid misunderstanding, *E/Z* nomenclature will be used to distinguish isomers around the carbon–carbon double bond, while *s-cis* and *s-trans* notation corresponds to different conformations caused by hindered rotation around central C–C bond in dienes.

Table 7. Relative Energies of Vinyl–Vinyl Coupling from [Pt^{IV}(*E/Z*)-CH=CH]₂L₄]²⁻ Complexes (in kcal/mol)^{a,b}

	<i>E/E</i>	<i>Z/E</i>	<i>Z/Z</i>
initial	0.0	10.7	21.9
TS	28.1	39.3	51.9
product	−6.5	−6.4	−6.6
ΔE^\ddagger	28.1	28.5	30.0
ΔE	−6.5	−17.2	−28.5

^a $\Delta E^\ddagger = E(\text{Init}) - E(\text{TS})$; $\Delta E = E(\text{Init}) - E(\text{Prod})$. ^b *Z/E* and *Z/Z* pathways calculated in this work; for *E/E* pathway, see ref 13.

are given in Figure 4 and the energies in Table 7. According to the structures presented in Figure 4, C–C bond formation takes place through similar three-centered transition states as discussed earlier (see Figure 1 and Figure 2). Vinyl–vinyl coupling of the ligands with *E/E*, *Z/E*, and *Z/Z* stereochemistry does not deviate significantly from each other in the activation barriers, which are in the range of 28.1–30.0 kcal/mol (Table 7). Obviously, the stereochemistry of the reaction is not controlled kinetically. To the contrary, the increase of the relative energy of both initial bis- σ -vinyl derivatives and transition states in the order of *E/E* < *Z/E* < *Z/Z* indicates thermodynamic control of the process. Each (*Z*)- σ -vinyl ligand substitution from (*E*)- σ -vinyl disfavors thermodynamic stability by ~10 kcal/mol.

The origin of the thermodynamic control becomes clear if we closely examine the geometries of the transition states for all three coupling pathways. Since, the geometry around the double bond is rigid in the case of (*Z*)- σ -vinyl ligand, the bulky iodine atom on vinyl is much closer to the ligands on the metal than for (*E*)- σ -vinyl ligand. This causes a steric repulsive energy of 11–12 kcal/mol. Of course, the same is also applicable to the initial bis- σ -vinyl complexes as well. Releasing of this strain energy on the product stage leads to higher exothermicity in the order *Z/Z* > *Z/E* > *E/E* by approximately the same value of ~12 kcal/mol (Table 7). Thus, in full agreement with experimental findings, the (*E/E*)-vinyl–vinyl coupling pathway is the most favored one in the present system. The higher reactivity of *E* isomers has been also observed in the palladium-catalyzed vinyl–vinyl cross-coupling reaction.⁷⁶ The conclusions made in the present work are also in agreement with another experimental observation, which detected both *E* and *Z* isomers for triple bond activation in a similar PdCl₂/Cl⁻ system.⁷⁷ Obviously, the smaller size of the chlorine atom compared to iodine decreases possible repulsive interactions and thus leads to a *Z/E* isomer mixture.

To summarize, rigid geometry around the carbon–carbon double bond allows stereoselectivity control of the vinyl–vinyl coupling stage via adjusting steric interaction between the vinyl ligand and metal coordination sphere.

F. Asymmetric Nature of Vinyl–Vinyl Coupling. After careful consideration of the vinyl–vinyl reductive elimination reaction, we have found that C–C bond formation through the *s-trans* pathway may proceed via two different transition states representing nonsuperimposable mirror image structures. Figure 6 shows an example corresponding to the experimentally observed C–C coupling reaction discussed above (see the section Steric Effect Induced by Substituents on Vinyl Groups).

(76) Abarbri, M.; Parrain, J.-L.; Cintrat, J.-C.; Duchene, A. *Synthesis* **1996**, 82.

(77) Bäckvall, J.-E.; Nilsson, Y. I. M.; Gatti, R. G. P. *Organometallics* **1995**, *14*, 4242.

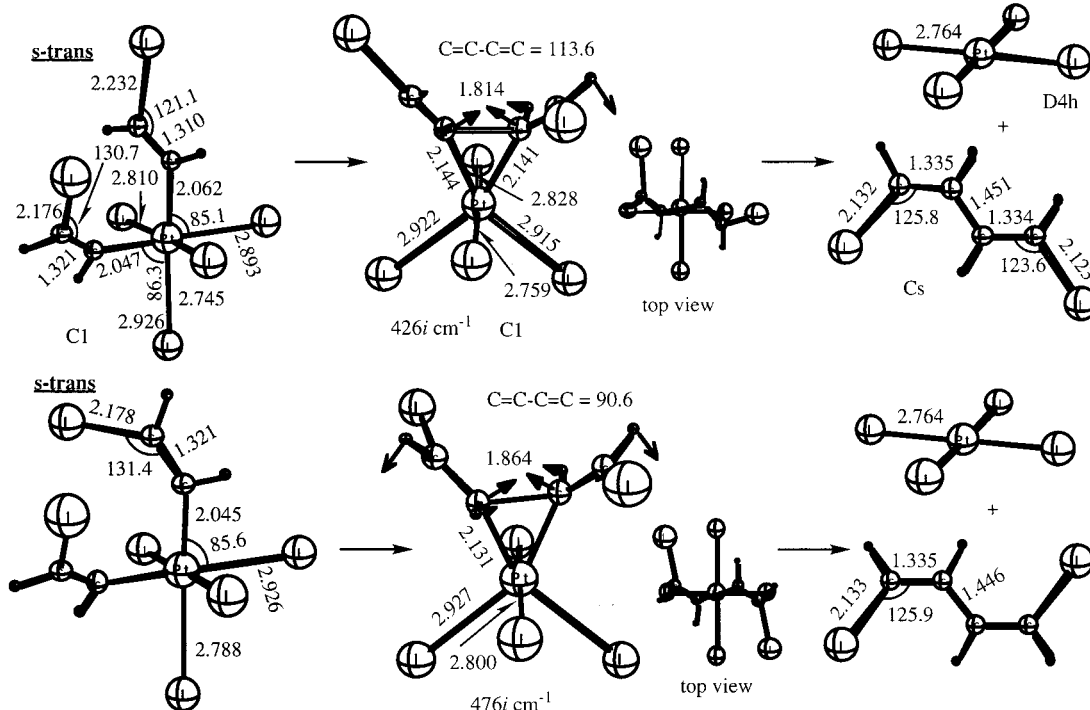


Figure 4. Optimized structures for Z/E (top) and Z/Z (bottom) coupling reactions.

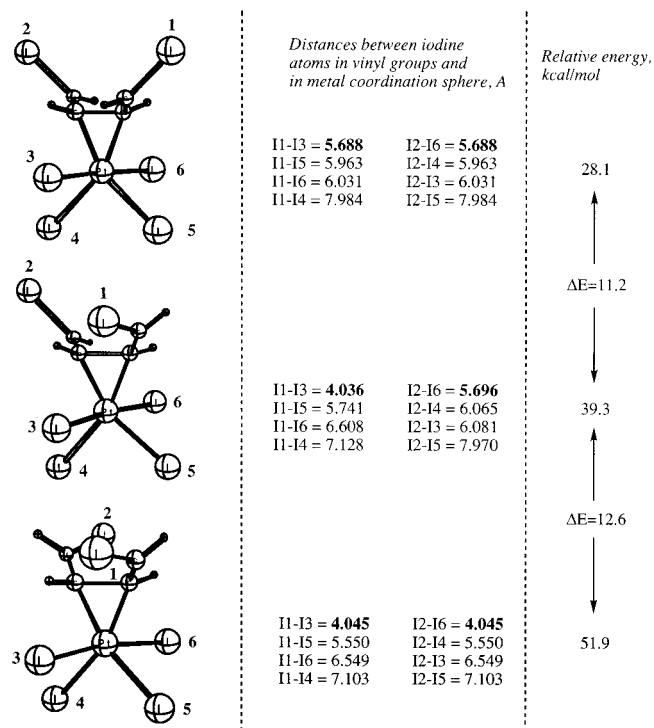


Figure 5. Some selected geometry parameters and relative thermodynamic stability of E/E (top), Z/E (middle), and Z/Z (bottom) coupling transition states.

Backward IRC calculations lead to nonsuperimposable bis- σ -vinyl initial complexes related to each other as mirror images. Of course, as enantiomeric structures, both transition states and both initial complexes have exactly the same energy and geometry parameters and are indistinguishable by any other scalar properties. Forward IRC calculations in both cases result in the same final product. In contrast to the s-trans pathway, reductive elimination through the s-cis pathway does not exhibit

enantiomeric variations (i.e., mirror images of transition state and initial complex are superimposable).

Thus, the present studies revealed that the vinyl–vinyl reductive elimination reaction may proceed through two enantiomeric (s-trans) and one meso (s-cis) pathways.⁷⁸ These investigations give important information for further experimental research. Within this C–C reductive elimination scheme, one can facilitate either enantiomeric or nonenantiomeric routes simply by adjusting the structure of σ -vinyl ligands.

As seen in Figure 6A, the principal structural unit responsible for chirality in the studied system consists only of vinyl groups and the metal atom; thus, any coupling reaction through the three-centered s-trans reductive elimination transition state would allow an existence of two enantiomeric pathways.⁷⁹ The question of chirality in the studied system is closely related to symmetry: The C_2 pathway exhibits enantiomeric properties, while C_s does not. The finding is in agreement with the C_2 symmetry design concept used in asymmetric catalysis for a long time.^{14,80,81} Available experimental study does not provide evidence for the presence of chiral asymmetric catalysis, since it was based on simple compounds without asymmetric properties. However, the feature may be employed, providing more complicated asymmetric substrates and ligands.

G. Comparison of ΔH and ΔG Energy Surfaces. The calculations given in Table 1 showed that ΔE reproduces ΔH both in reaction and in activation energies within 2 kcal/mol differences. Concerning the Gibbs free energy surface, ΔG^\ddagger

(78) Valid in the case of symmetric ligand environment (C_2 for s-trans and C_s for s-cis); for nonsymmetrical C_1 coupling (for example, with Z/E type of initial complexes) both s-trans and s-cis pathways will have enantiomeric pairs.

(79) See Figure S3 in Supporting Information for enantiomeric structures corresponding to reductive elimination from typical square planar and octahedral complexes.

(80) Whitesell, J. K. *Chem. Rev.* **1989**, *89*, 1581.

(81) Helmchen, G.; Pfaltz, A. *Acc. Chem. Res.* **2000**, *33*, 336. (b) Hayashi, T. *Acc. Chem. Res.* **2000**, *33*, 354.

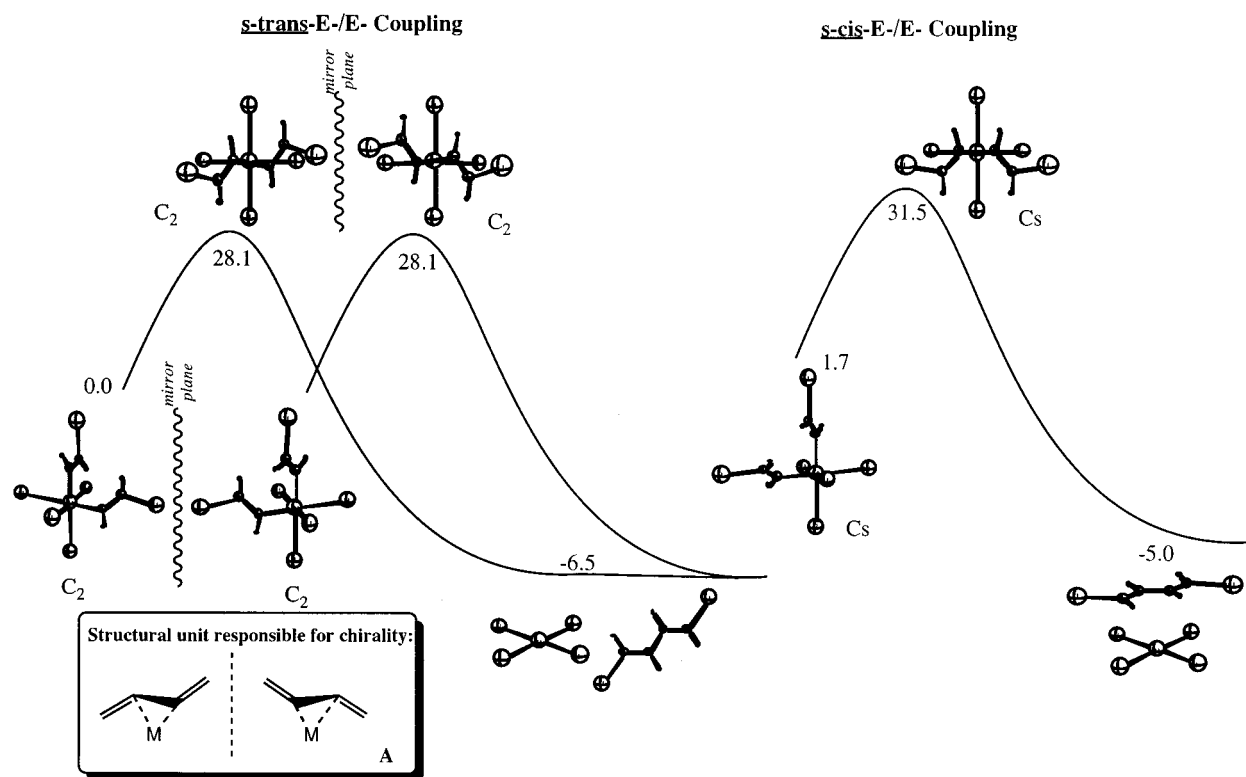


Figure 6. Reductive elimination through the *s*-trans and *s*-cis pathways (energy in kcal/mol).

values faithfully agree with ΔE^\ddagger and ΔH^\ddagger within the same small range of ~ 2 kcal/mol. The same is applicable for ΔG as well, except for the stage involving dissociation. For the latter case, the processes become more exothermic by 7–13 kcal/mol. This is an expected difference, due to entropy contribution. To summarize, ΔE values were found reliable in all cases and can be used to construct potential energy surfaces without further increasing of computational cost. The entropy contribution favors 1,3-diene dissociation by ~ 10 kcal/mol.

H. Comparison the Vinyl–Vinyl (C_{sp^2} – C_{sp^2}) and Alkyl–Alkyl (C_{sp^3} – C_{sp^3}) Reductive Elimination. Comparing C_{sp^2} – C_{sp^2} reductive elimination with the similar process involving alkyl groups (C_{sp^3} – C_{sp^3}), one may clearly note the same qualitative trends. Experimental studies have shown that dimethyl complexes of palladium(II) eliminate ethane much easier than their platinum(II) analogues,^{23,28} and reactivity of platinum(IV) methyl complexes is higher than platinum(II).²³ These results are in line with our findings (Table 1).

However, the absolute values of activation energies computed for vinyl–vinyl coupling are significantly lower than that for methyl–methyl coupling. Particularly, $\Delta E^\ddagger = 49.8$ kcal/mol (MP4//MP2 level),^{32a} $\Delta E^\ddagger = 60.8$ kcal/mol (MP4//HF),^{32b,c} and $\Delta H^\ddagger = 41.1$ kcal/mol (GVB)^{30a} were reported for ethane reductive elimination from $[\text{Pt}^{\text{II}}(\text{CH}_3)_2(\text{PH}_3)_2]$. The values are much higher than $\Delta E^\ddagger = 19.3$ kcal/mol ($\Delta H^\ddagger = 18.2$ kcal/mol) calculated in the present work for vinyl–vinyl coupling from $[\text{Pt}^{\text{II}}(\text{CH}=\text{CH}_2)_2(\text{PH}_3)_2]$. Ethane elimination from $[\text{Pd}^{\text{II}}(\text{CH}_3)_2(\text{PH}_3)_2]$ was found to proceed with $\Delta H^\ddagger = 10$ kcal/mol (GVB)^{30a} and $\Delta E^\ddagger = 26.3$ kcal/mol (MP4//HF),^{32c} while our value for $[\text{Pt}^{\text{II}}(\text{CH}=\text{CH}_2)_2(\text{PH}_3)_2]$ is again lower $\Delta E^\ddagger = 6.8$ kcal/mol ($\Delta H^\ddagger = 5.9$ kcal/mol). Similar relationships are found for the ethane reductive elimination from $[\text{Rh}^{\text{III}}(\text{CH}_3)_2(\text{PH}_3)\text{Cp}]$, $\Delta E^\ddagger = 65.6$ kcal/mol (MP2//HF),³⁶ and $[\text{Pt}^{\text{IV}}(\text{CH}_3)_2(\text{PH}_3)_2\text{Cl}_2]$,

$\Delta H^\ddagger = 34.2$ kcal/mol (GVB),^{30a} as compared to $[\text{Rh}^{\text{III}}(\text{CH}=\text{CH}_2)_2(\text{PH}_3)_2\text{Cl}]$, $\Delta E^\ddagger = 17.8$ kcal/mol, and $[\text{Pt}^{\text{IV}}(\text{CH}=\text{CH}_2)_2(\text{PH}_3)_2\text{Cl}_2]$, $\Delta H^\ddagger = 17.5$ kcal/mol, given in the present work. In addition, vinyl–vinyl coupling is generally much more exothermic than methyl–methyl coupling.^{30a,32,36} The differences may come from the relative stability in the products; $D(\text{C}–\text{C})$ in buta-1,3-diene, 115.8 kcal/mol,⁵⁹ is considerably larger than in ethane, 90.0 kcal/mol,⁸² thus making vinyl–vinyl coupling energetically favored compared to methyl–methyl reductive elimination. These theoretical results fairly well agree with experimental findings, which point out that practical implementation of C_{sp^3} – C_{sp^3} coupling is rather problematic due to slow reductive elimination,⁸³ in contrast to the processes involving vinyl groups.

I. Solvent Effect on the Vinyl–Vinyl Coupling Reaction.

Recently, we showed that solvent effect may play a crucial role in the mechanism of chemical reactions involving charged transition metal complexes.¹³ To take into account the possible solvent effect of polar media for the present reaction, we performed PCM calculations modeling the water environment for all the C–C coupling reactions (Table 1). Comparing ΔG energy surfaces in gas phase and in water, the following trends may be outlined: (i) Solvation does not affect in a substantial manner the processes involving neutral complexes with PH_3 or NH_3 ligands (**4**, **5**, **9**, **10**, **13**, **17–22**), the average energy changes are ~ 2 – 3 kcal/mol, and (ii) a polar surrounding greatly facilitates reductive elimination from the dianionic derivatives (**1–3**, **6–8**, **11**, **12**, **14–16**) by reducing, on average, activation

(82) *CRC Handbook of Chemistry and Physics 1999–2000*, 80th ed.; Lide, D. R., Ed.; CRC Press: Boca Raton, 1999; pp 9-65–9-66.

(83) Knochel, P. In *Metal-Catalyzed Cross-Coupling Reactions*; Diederich, F., Stang, P. J., Eds.; Wiley-VCH: Weinheim, Germany, 1998; pp 387–419.

energies by 8 kcal/mol and increasing reaction exothermicity by 10 kcal/mol; also, significant stabilization (~ 30 kcal/mol) occurs for zerovalent palladium and platinum derivatives $[\text{MX}_2]^{2-}$ (6–8, 14–16).

These trends can be rationalized that, in the dianionic systems studied, electrostatic interactions make a dominant contribution into the PCM solvation energy (usually $>90\%$). In these complexes, the charge is mainly located on the halogen atoms, and therefore, removing the shielding σ -vinyl groups upon reductive elimination increases the solvent-accessible area to the negative charge, thus favoring solvation. This effect is expected to be maximized in the product.

Conclusions

From the above presented studies one can draw the following conclusions

(i) If the same ligand environment is used, the electronic factors suggest the following relative activity in the vinyl–vinyl reductive elimination reaction: $\text{Pd}^{\text{II/IV}} > \text{Pt}^{\text{II/IV}}$, $\text{Ru}^{\text{II}} > \text{Os}^{\text{II}}$, $\text{Rh}^{\text{III}} > \text{Ir}^{\text{III}}$. In all the cases studied here, the lighter metal in each subgroup was found to be more active. Among all studied complexes, the Pd complexes are suggested to be the most active for the vinyl–vinyl coupling reaction.

(ii) Rather complicated ligand dependence of the reaction energetics can be expected due to competition between the electronic and steric effects. For the set of ligands studied here, the electronic and steric factors favoring the reductive elimination reaction decrease in the order, $\text{PH}_3 > \text{NH}_3 > \text{halogens}$ and $\text{I} > \text{Br} > \text{Cl} > \text{NH}_3, \text{PH}_3$, respectively, and results in the following activity order in C–C bond formation process, $\text{PH}_3 > \text{I} > \text{Br}, \text{NH}_3 > \text{Cl}$.

(iii) Besides the energetic and structural properties, two other unique features of the vinyl–vinyl coupling process are reported: (a) steric effect induced by substituents in vinyl groups, which would allow easy stereoselectivity control, and (b) asymmetric nature of vinyl–vinyl coupling, which, in turn, can also be controlled by adjusting structural parameters.

(iv) The solvent effect study has shown that halogen complexes may undergo a reductive elimination reaction much easier in a polar medium. An advantage of derivatives with phosphine ligands is that they can be used in both polar and nonpolar solvents.

To the best of our knowledge, this work is the first comprehensive computational study of the vinyl–vinyl coupling reaction. However, this work left unanswered the questions related to the role of the steric and electronic effects of the substituents on phosphorus ligands (PPh_3 , etc.) and the mechanism of reductive elimination from complexes with coordination vacancies. These questions are a subject of ongoing work and will be reported elsewhere.

Acknowledgment. V.P.A. acknowledges the Visiting Fellowship from the Emerson Center. The present research is in part supported by a grant (CHE-9627775) from the National Science Foundation. Acknowledgment is made to the Cherry L. Emerson Center of Emory University for the use of its resources, which is in part supported by a National Science Foundation grant (CHE-0079627) and an IBM Shared University Research Award.

Note Added after ASAP: There was an error in Table 1 in the version posted ASAP February 26, 2002; the corrected version was posted March 13, 2002.

Supporting Information Available: Figure S1: the normal-mode vector corresponding to changing buta-1,3-diene coordination from $\eta^2\text{-C-C}$ to $\eta^2\text{-C=C}$ type. Figure S2: the definition of the dihedral angle between M–X and C–C planes for square planar M^{II} and octahedral M^{IV} complexes. Figure S3: enantiomeric structures of initial bis- σ -vinyl complexes and reductive elimination transition states for a typical square planar and octahedral geometry (PDF). This material is available free of charge via the Internet at <http://pubs.acs.org>.

JA017476I